A POSITIVE MOMENT REPRESENTATION FOR THE ANGULAR FOKKER-PLANCK OPERATOR

A Thesis

Submitted to the Graduate Faculty of the

Louisiana State University and

Agricultural and Mechanical College

in partial fulfillment of the

requirements for the degree of

Master of Science in Nuclear Engineering

in

The Department of Nuclear Science

by

Mark Landesman

B.S., Louisiana State University, 1984

December 1986

Acknowledgements

I would like to thank my entire family for their help and encouragement during my education. Special thanks go to my mother, who saw me through the worst times with unfailing support. I appreciate the use of Los Alamos National Laboratory's magnificent computer and other technical facilities. I wish to extend my gratitude to Dr. Mark L. Williams and Dr. J. C. Courtney of LSU for their assistance in my graduate education. I am particularly grateful to Dr. J. E. Morel of Los Alamos National Laboratory for his supervision of the research and writing of this thesis and for his (almost) infinite patience.

Contents

List of Tables

List of Figures

Abstract

Traditional methods of performing transport calculations with forward peaked cross sections represent the wide angle scattering with Legendre polynomials and the small angle scattering with a finite difference approximation to the Fokker-Planck operator. Finite difference representations being incompatible with standard discrete ordinates codes, Morel has derived a moment expansion for use in Boltzmann calculations which rigorously approximates the Fokker-Planck operator but gives a scattering matrix with some negative elements. In certain types of problems, these negative elements result in negative angular fluxes. Conversely, the standard finite difference approximation gives a positive scattering matrix and, hence, always gives positive angular flux solutions. In order to retain compatibility with existing Sn codes and obtain a positive approximation to the Fokker-Planck operator, we have modified the expansion moments in a least squares fashion constrained to give a positive angular scattering matrix and preserve the momentum transfer. The resultant scattering matrix closely approximates the finite difference representation. The given modified cross section moments representative of small angle scattering have the advantages of moment operators and finite difference operators in that they can be used in standard Sn codes and guarantee positive flux solutions. The modified scattering matrix contains small wide angle scattering elements which are not present in the tridiagonal finite difference operator. In the typical case where smooth and forward peaked scattering is present, the smooth scattering expansion dominates the small differences in the scattering matrices. Boltzmann-Fokker-Planck calculations using the scattering matrices generated with the two different methods have essentially identical, positive solutions.

Chapter 1

Introduction

1.1 Objectives

The Boltzmann transport equation[1] is a mathematical description for a differential balance of particles that interact with the medium in which they travel. A simplified version of it and a description of the terms contained in it are in the Appendix. Although the transport equation is relatively simple to derive, it is impossible to solve analytically for all but the simplest problems. Solutions are obtained via different numerical schemes that have been developed over the last thirty years. These schemes can be grouped into stochastic and deterministic methods. Stochastic methods solve the transport equation by tracing the history of interactions of many particles as they travel through the medium. Deterministic methods solve for the expected (i.e. average) distribution without accounting for the statistical variations. One of the most common of the deterministic methods is called the "discrete ordinates" method because it discretizes the phase–space continuum into a space–energy–direction mesh and "transports" the particles from one mesh cell to the next using finite

probabilities calculated from the material and geometric data[2].

One of the characteristics of most of the computer codes that use discrete ordinates is their calculation of the discrete angle–to–angle scattering probability based on Legendre expansions of the differential scattering cross section. The required cross section data for these codes is simply the Legendre moments of the scattering function. For many scattering distributions, low order expansions produce sufficiently accurate results. However, with the developments in charged particle transport, interest has grown in the solution of the transport equation for cases when the scattering is highly forward peaked. Increasingly forward peaked scattering distributions require increasingly higher order expansions to accurately represent them. Truncation of the expansion at an insufficiently high order causes the expansion to oscillate about the true distribution in the region of large angle scatter. If the scattering probability is small in this region, the oscillatory nature of Legendre polynomials can cause the expansion to oscillate negatively as in Figure 1.1 . This region of the cross section expansion would represent a negative probability of scatter, which is nonphysical. In the discretized form used by computer programs, this can cause the angle–to–angle scattering elements to be negative. For certain classes of problems this may lead to negative flux solutions, which are also nonphysical. This could be corrected by using an orthogonal set of polynomials other than the Legendre polynomials to expand the cross section or by representing the cross section by some other method such as with a set of discrete values. The disadvantage in either of these (or any other) method is that it would require development of an entirely new set of transport codes that could use such data. The codes presently in use require that the cross section be represented by a Legendre expansion and that the input be the Legendre moments of the cross section . These codes are extremely versatile and have been extensively verified. Instead of developing a set of programs to handle the

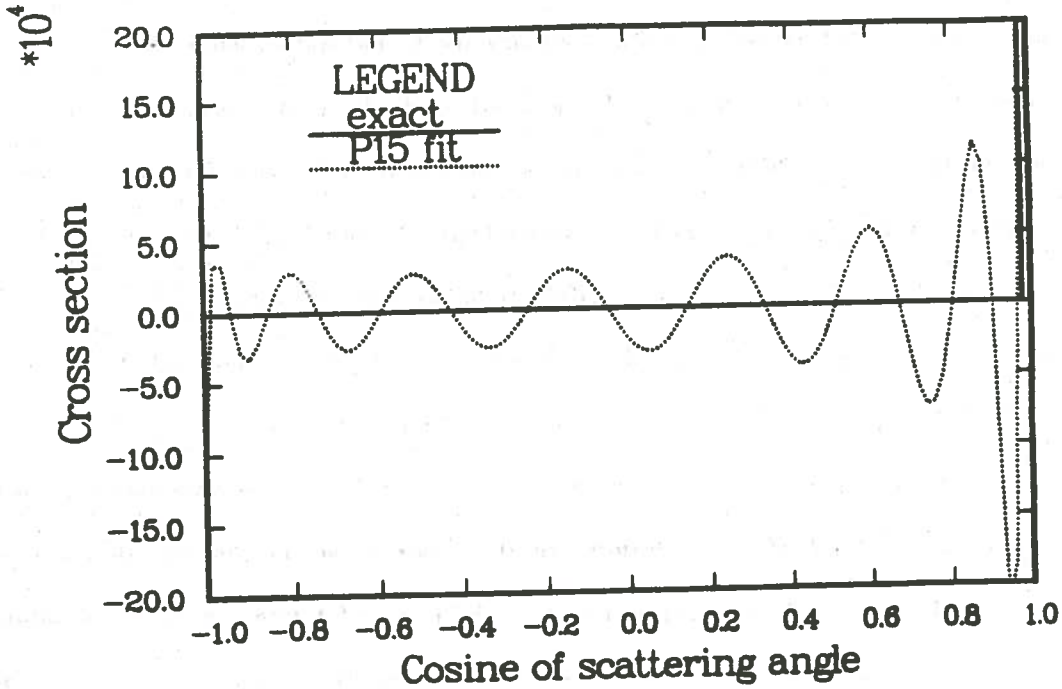

Figure 1.1: Legendre expansion of a forward peaked cross section

small class of problems for which negative oscillations in the cross section cause trouble, it would be advantageous to develop a new set of Legendre moments that are modified in some fashion to guarantee a positive discrete angular scattering operator in contemporary discrete ordinates codes.

The objectives of this thesis are:

1. to develop a method of cross section moment modification which will guarantee positivity of the discrete angular scattering operator and be accurate for highly forward peaked scattering, and

2. to assess the accuracy of this method by comparison against a traditional approach which combines the Legendre moment representation with a finite difference Fokker-Planck approximation.

1.2 Representation of a forward peaked cross section

Any piecewise continuous function of one variable can be represented by an expansion in Legendre polynomials[3]. A drawback to this approach is that for increasingly biased functions, increasingly higher order expansions are required to accurately represent them over the full range of the expansion until, in the limiting case of a Dirac delta function, an infinite expansion order is required to represent it correctly.

Differential scattering cross sections used in calculations are functions of the cosine of the angle of scatter in the laboratory system and can be expanded in Legendre polynomials. The scattering distribution may vary in form from isotropic to extremely forward peaked for charged particles and high energy neutrons. Isotropic and slowly varying scattering probabilities can be accurately expanded in Legendre polynomials of low order. Cross sections typical of charged particle interactions may be difficult to accurately fit even using a fifteenth order Legendre expansion. The accuracy of the fit is biased toward the regions of small angle scatter (regions of largest cross section), degrading the fit in the wings (regions of wide angle scatter).

Since the forward peaked cross section is difficult to model over the full range, we can separate the cross section into two components, a smooth part and a forward peaked part, and treat each separately over the partial regions of the domain. Since it is slowly varying, the smooth cross section can be represented by a low order Legendre expansion using moments fit over the smooth region of the domain. This partial range fit of Legendre moments defeats the orthogonality property of the Legendre polynomials and requires special treatment which will be discussed later.

The forward peaked region of the cross section is still rapidly varying and is not amenable to representation by Legendre expansions. Traditional methods have included treating the

forward peaked scattering with a finite difference approximation to the Fokker-Planck operator. The Fokker-Planck operator, which is derived in the Appendix, assumes that grazing collisions are the dominant mode of scatter[4]. Grazing collisions incur small angular deflections and correspondingly small energy losses and are therefore forward peaked reactions. These methods of treating the forward peaked component of the scattering have a severe drawback. They use finite difference approximations which exclude the use of present discrete ordinates codes. A more efficient way of treating the forward peaked component would be to provide a set of moments representative of the Fokker-Planck operator as input to standard discrete ordinates codes. Morel has derived an expression for such a set of moments[5]. Since the Legendre polynomials are eigenfunctions of both operators, he equated the eigenvalues of the Boltzmann integral scattering operator to the Fokker-Planck differential scattering operator as they operated on the Legendre polynomials. The expression algebraically reduced to a polynomial expression for the moments linear in the momentum transfer. Unfortunately, Morel's moment representation for the Fokker-Planck operator is not positive. Expressions using these " Fokker-Planck equivalent" moments accurately represent the forward-peaked scattering, but oscillate about zero in the large scattering region in much the same way that truncated Legendre cross section expansions oscillate.

These negative oscillations in the cross section expansion can cause negative elements in the discrete Boltzmann scattering operator. This has little effect in most classes of transport problems since the negative elements are usually small compared to the forward peaked scattering elements. However, when solving certain cases of normally incident boundary sources, the reflected source is small enough that the contributions of the negative scattering array elements can dominate the solution at some of the discrete reflected directions. This is not seen when the boundary source is isotropically incident, since the scattering sources nearer

the reflected directions dominate the small negative reflected fluxes caused by the normally incident components. Thus, though there is a method of treating the Fokker-Planck component of the angular scattering source which is compatible with contemporary discrete ordinates computer programs, it can produce nonphysical solutions for certain classes of problems. This thesis presents a method of preventing these nonphysical solutions by modifying the forward peaked operator.

Chapter 2

The discrete ordinates scattering operator

2.1 Legendre expansions of cross sections

Since the Legendre polynomials form a complete basis that spans the space of all continuous functions defined over [-1,+1], any function of one variable can be expanded in Legendre polynomials. Scattering cross sections are isotropic in the azimuthal angle. They are a function of only the polar angle, θ, which can be represented uniquely by its cosine, which is defined over [-1,+1]. Therefore, scattering cross sections can be expanded in Legendre polynomials.

The exact expansion of a cross section in Legendre polynomials is

$$\sigma(\mu_o) = \sum_{\ell=0}^{\infty} \frac{2\ell+1}{2} \sigma_\ell P_\ell(\mu_o) \quad , \tag{2.1}$$

where the coefficient, σ_ℓ, is the ℓ^{th} Legendre moment. An infinite expansion, though it is

exact, is unfeasible. A more practical method is to truncate the expansion at order L and choose the Legendre moments such that the error, ϵ, defined by

$$\epsilon = \int_{-1}^{+1} [\sigma(\mu_o) - \sum_{\ell=0}^{L} \frac{2\ell+1}{2} \sigma_\ell P_\ell(\mu_o)]^2 d\mu_o \quad , \tag{2.2}$$

is a minimum. The error is minimized using the standard minimization technique of setting the derivative of the error with respect to each moment to zero:

$$\frac{\delta\epsilon}{\delta\sigma_\jmath} = 2\int_{-1}^{+1} [\sigma(\mu_o) - \sum_{\ell=0}^{L} \frac{2\ell+1}{2} \sigma_\ell P_\ell(\mu_o)] \frac{2\jmath+1}{2} P_\jmath(\mu_o) d\mu_o, \qquad \jmath = 0 \ldots L \tag{2.3}$$

$$= 0 \quad . \tag{2.4}$$

Rearranging equation 2.3 ,

$$\int_{-1}^{+1} \sigma(\mu_o) P_\jmath(\mu_o) d\mu_o = \int_{-1}^{+1} \sum_{\ell=0}^{L} \frac{2\ell+1}{2} \sigma_\ell P_\ell(\mu_o) P_\jmath(\mu_o) d\mu_o \quad , \tag{2.5}$$

the orthogonality property[6] of the Legendre polynomials can be invoked to reduce the right hand side of equation 2.5 to

$$\sum_{\ell=0}^{L} \frac{2\ell+1}{2} \sigma_\ell \frac{2}{2\jmath+1} \delta_{\ell\jmath} = \sigma_\jmath \quad . \tag{2.6}$$

Thus, for the error in the expansion to be a minimum, the cross section moments must be defined as

$$\sigma_\ell = \int_{-1}^{+1} \sigma(\mu_o) P_\ell(\mu_o) d\mu_o \quad . \tag{2.7}$$

Equation 2.2 requires that the Legendre moments of the error squared go to zero. This implies mean convergence, or that the average of the error over the full range of the expansion be zero. The error is not constrained to uniformity over the full range. The least squares procedure, in the absence of a weighting function, will fit the function better where it is largest. Consequently, the relative error can, and frequently does, become very small in some regions at the expense of the accuracy in other regions.

2.2 Discretization of the continuous scattering source

The Boltzmann scattering source for scattering from μ' to μ in one dimensional slab or spherical geometry is defined as

$$S(\mu) = \frac{1}{2\pi}\int_0^{2\pi}\int_{-1}^{+1}\sigma(\mu_o)\psi(\mu')d\mu' d\phi\prime, \tag{2.8}$$

where

$$\mu_o = \mu'\mu + \sqrt{(1-\mu'^2)(1-\mu^2)}cos\phi' \quad [7]. \tag{2.9}$$

By replacing the cross section with its Legendre expansion,

$$S(\mu) = \frac{1}{2\pi}\int_0^{2\pi}\int_{-1}^{+1}\sum_{\ell=0}^{L}\frac{2\ell+1}{2}\sigma_\ell P_\ell(\mu_o)\psi(\mu')d\mu' d\phi\prime, \tag{2.10}$$

and by invoking the spherical harmonics addition theorem[8], the scattering can be restated in terms of the initial and final direction cosines:

$$S(\mu) = \int_{-1}^{+1}\sum_{\ell=0}^{L}\frac{2\ell+1}{2}\sigma_\ell P_\ell(\mu)P_\ell(\mu')\psi(\mu')d\mu'. \tag{2.11}$$

After extracting all the elements independent of μ' from the integral,

$$S(\mu) = \sum_{\ell=0}^{L}\frac{2\ell+1}{2}\sigma_\ell P_\ell(\mu)\int_{-1}^{+1}P_\ell(\mu')\psi(\mu')d\mu', \tag{2.12}$$

all that remains in the integrand is the expression for the ℓ^{th}flux moment which is analogous to the ℓ^{th} cross section moment defined previously. Replacing the integral with the ℓ^{th}flux moment,

$$S(\mu) = \sum_{\ell=0}^{L}\frac{2\ell+1}{2}\sigma_\ell P_\ell(\mu)\phi_\ell, \tag{2.13}$$

the equation can be rearranged to group the flux and cross section moments:

$$S(\mu) = \sum_{\ell=0}^{L}\frac{2\ell+1}{2}P_\ell(\mu)[\sigma_\ell\phi_\ell]. \tag{2.14}$$

The product in brackets is the ℓ^{th}moment of the scattering source. The remainder of the right hand side of equation 2.14 is the Legendre expansion that maps the source from the moment basis to the discrete basis.

The analytical integral expression in equation 2.12 can be replaced with quadrature integration, giving

$$S(\mu) = \sum_{\ell=0}^{L} \frac{2\ell+1}{2} \sigma_\ell P_\ell(\mu) \sum_{i=1}^{M} P_\ell(\mu_i)\psi(\mu_i)\omega_i. \tag{2.15}$$

However, two conditions must be met in order for the integration in equation 2.15 to be exact. The first is that $\psi(\mu)$ must vary as a polynomial that can be uniquely defined by the M direction–flux (μ, ψ) pairs. This is required because standard quadratures can only exactly integrate polynomials. The second condition is that the quadrature order M must be sufficiently high for the quadrature to exactly perform the integration. The choice of M is dependent on the quadrature set. For example, Gaussian quadrature of order eight will exactly integrate a fifteenth order polynomial[9], whereas a ninth order Lobatto quadrature is required to perform the same integration exactly. As was stated previously, the numerical integration in equation 2.15 calculates the flux moments from the angular flux at discrete directions.

2.3 Matrix formulation of the scattering operator

The calculation of flux moments and re-expansion of the source represented by equation 2.15 is the standard method of performing scattering calculations in discrete ordinates methods. The summations in this equation can be represented by a series of matrix operations. Three matrix operators can be defined as:

1.

$$D_{kj} = P_\ell(\mu_j)\omega_j, \tag{2.16}$$

2.

$$\Sigma_{\ell k} = \sigma_\ell I_{\ell k}, \tag{2.17}$$

and

3.

$$M_{i\ell} = \frac{2\ell+1}{2} P_\ell(\mu_i). \tag{2.18}$$

The first operator, D_{kj} , is the discrete–to–moment operator that maps the discrete fluxes into the moment basis. The second operator, $\Sigma_{\ell k}$, is the diagonal matrix formed by the vector of cross section moments and the identity matrix, I. The third operator, $M_{i\ell}$, is the moment–to–discrete operator that maps the source moments into the discrete basis. The matrix equation for calculating the flux moment using the operator defined above would be

$$\phi_k = D_{kj}\psi_j. \tag{2.19}$$

The source calculation in the Legendre basis using matrix notation would be

$$s_\ell = \Sigma_{\ell k}\phi_k. \tag{2.20}$$

The discrete angular source would be calculated from the source in the moment basis by

$$S_i = M_{i\ell}s_\ell. \tag{2.21}$$

The discrete scattering source vector, S_i, due to a discrete angular flux vector, ψ_j, is

$$S_i = M_{i\ell}\Sigma_{\ell k}D_{kj}\psi_j \tag{2.22}$$

or

$$S_i = S_{ij}\psi_j, \tag{2.23}$$

where the discrete angular scattering operator for scattering from μ_j to μ_i is

$$S_{ij} = M_{i\ell}\Sigma_{\ell k}D_{kj}. \tag{2.24}$$

Chapter 3

A positive forward peaked scattering operator

In this chapter, the Fokker-Planck approximation to the one group transport equation is introduced. Then, a set of Fokker-Planck equivalent cross sections are developed as input to standard transport codes for solving problems with highly anisotropic scattering. Since the expansion of this type of cross section is typically not everywhere positive, a scheme for modifying them to obtain a positive discrete angular scattering operator based on a particular quadrature set is presented.

3.1 Historical perspective

The Fokker-Planck equation assumes that small angles of scatter and correspondingly small energy losses are the dominant modes of scatter. Such is the case with charged particles and high energy neutrons produced by fission and fusion. Charged particles (i.e. electrons)

scatter by coulombic interaction where the probability of energy loss varies inversely as the square of the energy loss. Small energy losses (and small angular deflections) are much more probable, which makes coulombic interactions good candidates for modelling with the Fokker-Planck equation.

Many methods have been developed for solving the Fokker-Planck equation in some restricted fashion. Corman et al. (1975) used a multigroup method to handle the particle slowing down and an ad hoc "flux limited" diffusion coefficient to approximate the angular redistribution[10]. Pomraning (1983) has formalised this approach and shown that Fokker-Planck and transport corrected treatments of the scattering kernel are equivalent[11]. The use of a diffusion coefficient restricts this method to treatment of problems without strong source anisotropy, which is an inherent feature of Fokker-Planck problems. Antal and Lee (1976) calculated integral quantities, such as charge and energy deposition, using discrete ordinates techniques[12]. They derived equations that suitably modeled the slowing down but neglected angular scattering. Similarly, Moses (1977) approximated the paths of the particles as straight lines[13]. This is suitable only for heavy charged particles. It also does not allow for angular redistribution, which is of primary importance in some problems. Haldy and Ligou (1977) derived a modified scheme which allowed the particles to scatter to new energies and angles, but only in an infinite medium[14]. Mehlhorn and Duderstadt (1980) derived finite difference equations for the Fokker-Planck scattering operator which they implemented in TIMEX. The modified program, TIMEX–FP, possessed all the versatility of the parent code[15]. The approach was somewhat awkward since it required internal modification of the program. These methods have addressed strictly Fokker-Planck scattering. The most complete treatment of forward-peaked scattering has been presented by Caro and Ligou (1983) who separated the scattering operator into the smooth and singular components[16].

They expanded the smooth operator in Legendre moments and used a finite difference approximation to the Fokker-Planck operator for the singular component. This was the first coupling of the Boltzmann and Fokker-Planck operators in the treatment of forward-peaked scattering. Although this method gives a complete treatment of the scattering operator, it requires the development of a separate set of Boltzmann-Fokker-Planck codes. Morel (1981, 1985) has derived an expression for a set of cross section moments which are "Fokker-Planck equivalent" and can be used as input for existing discrete ordinates programs[17,18]. Within group cross sections account for angular scattering while the group to group cross sections account for energy loss. Morel's method, therefore, provides a complete energy and angle representation of the Fokker-Planck equation and is still able to use the plethora of analytical and numerical techniques developed for neutron transport and implemented in standard Sn codes. However, as will be shown, the method can produce nonphysical solutions for certain types of problems.

3.2 The Fokker-Planck approximation

A detailed derivation of the one group Fokker-Planck equation is given in the Appendix. Only a brief description of it will be given here. Starting with the one group, time independant, one dimensional slab or spherical Boltzmann transport equation for a nonmultiplying medium,

$$\mu\frac{\partial\psi}{\partial x}+\sigma_t\psi=\frac{1}{2\pi}\int_0^{2\pi}\int_{-1}^{+1}\sigma_s(\mu_o)\psi(\mu')d\mu'd\phi'+\mathcal{Q}(\mu), \tag{3.1}$$

it can be reformulated in terms of the net inscatter,

$$\mu\frac{\partial\psi}{\partial x}+\sigma_a\psi=\Gamma_B\psi+\mathcal{Q}(\mu), \tag{3.2}$$

where

$$\Gamma_B \psi = \frac{1}{2\pi} \int_0^{2\pi} \int_{-1}^{+1} [\sigma_s(\mu_o)\psi(\mu') - \sigma_s(\mu_o)\psi(\mu)] d\mu' d\phi' \tag{3.3}$$

is the net inscatter and Γ_B is the Boltzmann integral scattering operator. The coordinate system is rotated, changing the integration coordinates from the laboratory system (μ', ϕ') to the scattering frame (μ_o, ϕ_o). Since the Fokker-Planck approximation applies when $\mu_o \approx 1$, the flux is expanded in a truncated Taylor's series about this direction and integrated over ϕ_o. The result is

$$\mu \frac{\partial \psi}{\partial x} + \sigma_a \psi = \Gamma_{F-P} \psi + Q(\mu), \tag{3.4}$$

where the Boltzmann integral operator has been replaced with Γ_{F-P}, the asymptotic Fokker-Planck differential operator , which is

$$\Gamma_{F-P} \psi = \frac{\alpha}{2} \frac{\partial}{\partial \mu} (1 - \mu^2) \frac{\partial \psi}{\partial \mu}, \tag{3.5}$$

where

$$\alpha = \int_{-1}^{+1} \sigma_s(\mu_o)[1 - \mu_o] d\mu_o. \tag{3.6}$$

The coefficient, α, is called the momentum transfer in charged-particle transport literature. It is called the transport corrected scattering cross section in neutron transport literature.

For the flux derivatives not to become inordinately large, the flux must vary sufficiently smoothly. Since the Fokker-Planck equation evolves from a truncated Taylor's series about $\mu_o = 1$, the approximation is only valid for $\mu_o \approx 1$. If the scattering is indeed highly forward peaked, the integrand in equation 3.3 will be small except near $\mu_o = 1$, where the Fokker-Planck equation is valid. In such a case, the two scattering operators, Γ_B and Γ_{F-P}, would closely approximate each other.

3.3 Fokker-Planck equivalent moments

Standard discrete ordinates codes require an excessive number of Legendre cross section moments to correctly represent Fokker-Planck scattering. To correctly model the Fokker-Planck region using Legendre cross sections moments requires a much larger expansion order than a fit that ignores the accuracy in the regions of low probability scatter. Since the asymptotic Fokker-Planck scattering operator is accurate only for scattering through very small angles, equating it with the moment representation of the Boltzmann scattering operator will give a means of deriving a set of cross section moments which are "Fokker-Planck equivalent".

Since the Legendre polynomials form the basis of the flux expansion, they can be operated on with the Boltzmann scattering operator, giving

$$\Gamma_B P_\ell(\mu) = \frac{1}{2\pi}\int_0^{2\pi}\int_{-1}^{+1}\sigma_s(\mu_o)[P_\ell(\mu') - P_\ell(\mu)]d\mu' d\phi'. \tag{3.7}$$

After expanding the cross section in Legendre polynomials , equation 3.7 can be written

$$\Gamma_B P_\ell(\mu) = \frac{1}{2\pi}\int_0^{2\pi}\int_{-1}^{+1}\sum_{n=0}^{\infty}\frac{2n+1}{2}\sigma_n P_n(\mu_o)[P_\ell(\mu') - P_\ell(\mu)]d\mu', \tag{3.8}$$

where the cross section moments are defined as:

$$\sigma_n = \int_{-1}^{+1}\sigma(\mu_o)P_n(\mu_o)d\mu_o. \tag{3.9}$$

Using the spherical harmonics addition theorem to expand $P_n(\mu_o)$ and performing the integration in equation 3.8 yields

$$\Gamma_B P_\ell(\mu) = [\sigma_\ell - \sigma_0]P_\ell(\mu). \tag{3.10}$$

Similarly operating on the Legendre polynomials with the Fokker-Planck scattering operator,

$$\Gamma_{F-P} P_\ell(\mu) = \frac{\alpha}{2}\frac{\partial}{\partial\mu}\{[1-\mu^2]\frac{\partial P_\ell(\mu)}{\partial\mu}\}, \tag{3.11}$$

the outer derivative operation can be distributed to provide the following expression,

$$\Gamma_{F-P} P_\ell(\mu) = \frac{\alpha}{2}\{[1-\mu^2]\frac{\partial^2 P_\ell(\mu)}{\partial \mu^2} - 2\mu\frac{\partial P_\ell(\mu)}{\partial \mu}\}. \tag{3.12}$$

Using the recurrence relation for Legendre polynomials[19],

$$[1-\mu^2]\frac{\partial^2 P_\ell(\mu)}{\partial \mu^2} - 2\mu\frac{\partial P_\ell(\mu)}{\partial \mu} + \ell[\ell+1]P_\ell(\mu) = 0, \tag{3.13}$$

the right hand side of equation 3.12 can be replaced, providing the following simple expression:

$$\Gamma_{F-P} P_\ell(\mu) = -\frac{\alpha}{2}\ell[\ell+1]P_\ell(\mu). \tag{3.14}$$

Since Γ_B and Γ_{F-P} are to be equivalent operators, they are equated as they operate on the Legendre polynomials :

$$\Gamma_B P_\ell(\mu) = \Gamma_{F-P} P_\ell(\mu). \tag{3.15}$$

Substituting in equations 3.10 and 3.14 for $\Gamma_B P_\ell(\mu)$ and $\Gamma_{F-P} P_\ell(\mu)$, respectively:

$$[\sigma_\ell - \sigma_0]P_\ell(\mu) = -\frac{\alpha}{2}\ell[\ell+1]P_\ell(\mu), \qquad \ell = 0,\ldots,\infty \quad , \tag{3.16}$$

a simple expression for σ_0 can be derived algebraically:

$$\sigma_0 = \sigma_\ell + \frac{\alpha}{2}\ell[\ell+1], \qquad \ell = 0,\ldots,\infty \quad . \tag{3.17}$$

As the expansion order increases, σ_0 increases without limit. Truncating the expansion at order L and setting $\sigma_L = 0$ to minimize σ_0, it is found that

$$\sigma_0 = \frac{\alpha}{2}L[L+1], \tag{3.18}$$

and

$$\sigma_\ell = \sigma_0 - \frac{\alpha}{2}\ell[\ell+1], \qquad \ell = 0,\ldots,L \quad , \tag{3.19}$$

which can be rewritten

$$\sigma_\ell = \frac{\alpha}{2}\{L[L+1] - \ell[\ell+1]\}, \qquad \ell = 0, \ldots, L \quad . \tag{3.20}$$

Selection of the expansion order, L, and determination of the momentum transfer, α, from the cross section data determines the cross section moments representative of Fokker-Planck scattering. When using an expansion of order L, the Boltzmann integral operator is equivalent to the Fokker-Planck differential operator when operating on polynomials of order L or less.

An obviously desirable characteristic of the Fokker-Planck operator is that it be spherical harmonic equivalent. This property can be insured by applying certain restrictions to its usage. Having established the equivalence of Γ_B and Γ_{F-P} when operating on polynomials of order L or less with cross section expansions of order L, it logically follows that if Γ_B is somehow made spherical harmonic equivalent, then Γ_{F-P} must also be spherical harmonic equivalent under the same conditions. The spherical harmonic form of Γ_B in one dimensional slab or spherical geometry is

$$\Gamma_B \psi_p(\mu) = \sum_{\ell=0}^{N-1} \frac{2\ell+1}{2} \sigma_\ell \phi_\ell P_\ell(\mu) - \sigma_0 \psi_p(\mu), \tag{3.21}$$

where ϕ_ℓ is defined as

$$\phi_\ell = \int_{-1}^{+1} \psi_p(\mu) P_\ell(\mu) d\mu, \qquad \ell = 0, N-1. \tag{3.22}$$

If $\psi_p(\mu)$ is a polynomial of order $N-1$ or less, the integrand in equation 3.22 is a polynomial of order $2N-2$ or less which can be exactly integrated using the quadrature approximation

$$\phi_\ell = \sum_{i=1}^{N} \psi_p(\mu_i) P_\ell(\mu_i) \omega_i \tag{3.23}$$

if $\{\mu_i\}_{i=1}^N$ and $\{\omega_i\}_{i=1}^N$ are the Gauss quadrature zeroes and weights. Substituting equa-

tion 3.23 into equation 3.21 , we obtain the discrete ordinates form of Γ_B:

$$\Gamma_B\psi_p(\mu) = \sum_{\ell=0}^{N-1} \frac{2\ell+1}{2}\sigma_\ell[\sum_{i=1}^{N}\psi(\mu_i)P_\ell(\mu_i)\omega_i]P_\ell(\mu) - \sigma_0\psi_p(\mu), \tag{3.24}$$

where the expression in brackets exactly calculates the Legendre moment of the flux if μ_i and ω_i correspond to the Gaussian zeroes and weights. Using cross section expansions of order $N-1$ insures an expansion order equal to that of the spherical harmonics equations of order $N-1$. Thus, using Gauss quadrature of order N and cross section expansions or order $N-1$ when operating on polynomials of order $N-1$, the spherical harmonics form is equivalent to the discrete ordinates form of the Boltzmann scattering operator in one dimensional slab or spherical geometry and, hence, also to the Fokker-Planck operator.

Some final comments on the Fokker-Planck equivalent cross sections are warranted before continuing to the final section of this chapter. Recalling the definition of the momentum transfer,

$$\alpha = \int_{-1}^{+1}\sigma(\mu_o)[1-\mu_o]d\mu_o, \tag{3.25}$$

and substituting the appropriate Legendre polynomials ,

$$\alpha = \int_{-1}^{+1}\sigma(\mu_o)[P_0(\mu_o) - P_1(\mu_o)]d\mu_o, \tag{3.26}$$

the following simple expression for the momentum transfer results:

$$\alpha = [\sigma_0 - \sigma_1]. \tag{3.27}$$

Substituting the derived expressions for the Fokker-Planck moments into equation 3.27 :

$$\begin{aligned}\alpha &= \frac{\alpha}{2}L[L+1] - \frac{\alpha}{2}\{L[L+1]-2\} \qquad (3.28)\\ &= \alpha,\end{aligned}$$

it is shown that the momentum transfer is exact and independant of the expansion order.

Expressing the average cosine of the scattering angle as

$$\overline{\mu_o} = \frac{\sigma_1}{\sigma_0}, \tag{3.29}$$

and substituting the expressions for σ_0 and σ_1,

$$\begin{aligned} \overline{\mu_o} &= \frac{\frac{\alpha}{2}\{L[L+1]-2\}}{\frac{\alpha}{2}L[L+1]} && (3.30) \\ &= \frac{L[L+1]-2}{L[L+1]}, && (3.31) \end{aligned}$$

it is readily seen that $\overline{\mu_o}$ goes to one as the expansion order goes to infinity. The expression for the momentum transfer can be rewritten in terms of σ_0 and $\overline{\mu_o}$:

$$\begin{aligned} \alpha &= [\sigma_0 - \sigma_1] \\ &= \sigma_0[1 - \frac{\sigma_1}{\sigma_0}] && (3.32) \\ &= \sigma_0[1 - \overline{\mu_o}]. && (3.33) \end{aligned}$$

If the momentum transfer is to remain constant as the expansion order increases (and $\overline{\mu_o}$ approaches one) the scalar cross section must approach infinity. Upon examination of the expression for the scalar cross section ,

$$\sigma_0 = \frac{\alpha}{2}L[L+1], \tag{3.34}$$

σ_0 obviously varies as L^2 . The conclusions of this analysis are:

1. as the expansion order increases, the approximation made in deriving the Fokker-Planck equation ($\mu_o \approx 1$) becomes more accurate, and

2. in the Fokker-Planck limit, the scattering cross section becomes infinite, causing the particles to scatter continuously, but through a differentially small angle in each collision.

3.4 Approach to ensuring positivity

The Fokker-Planck equation is derived under the assumption of predominantly forward peaked scattering. No other assumptions are made regarding the angular distribution of the scattering. Hence, an expansion using the moments which represent a least squares fit to the Fokker-Planck scattering operator will produce a cross section that is forward peaked, but since it is a least squares fit, the accuracy will not necessarily be uniform. The regions of large cross section have a least squares weighting that is implicitly larger than the regions of small cross section . This heavier weighting causes the least squares fit to be better in the regions of larger cross section . To minimize the square of the average error, the moment expansion will oscillate about the actual function. In the region of large angle scatter of a forward-peaked cross section , the magnitude of the cross section is small enough that the oscillations can dominate the fit. Thus, this approach suffers from the same negative oscillations as in any forward peaked expansion. Recalling the Legendre expansion of the scattering source:

$$S(\mu) = \sum_{\ell=0}^{L} \frac{2\ell+1}{2} \sigma_\ell P_\ell(\mu) \sum_{i=1}^{M} P_\ell(\mu_i)\psi(\mu_i)\omega_i, \tag{3.35}$$

truncation of the expansion at an order L that is insufficiently high for properly representing the scattering cross section can cause $S(\mu)$ to oscillate negatively over part of the expansion. In the matrix formulation of equation 3.35 used by discrete ordinates,

$$S_i = S_{ij}\psi_j, \tag{3.36}$$

where

$$S_{ij} = M_{i\ell}\Sigma_{\ell k}D_{kj}, \tag{3.37}$$

negative oscillations in the Legendre expansion of the cross section may cause elements of this matrix operator to be negative. These negative elements, when folded with a positive

angular flux vector, may introduce a negative scattering source in some directions which may lead to a negative flux solution. The scheme presented in this section attempts to generate a set of modified cross section moments that will produce an angle–to–angle scattering operator that is positive at all the quadrature directions.

The negative elements in the scattering matrix have a complicated origin. The elements themselves are discrete values of a continuous product of two functions corresponding to the moment expansion of the cross section and the expansion basis of the flux. The flux expansion basis is inherent in the quadrature data which defines the discrete angular directions of the solution. Since the directions are chosen by the quadrature, which determines the accuracy of the flux solution, they are necessarily fixed. The flexibility in generating a positive scattering matrix lies in the option of modifying the moment representation of the cross section, which must be done with caution.

The method presented in this thesis attempts to modify the Fokker-Planck equivalent cross section moments subject to the following constraints:

1.

$$S_{i,j} = M_{i\ell}\Sigma^*_{\ell k}D_{kj} \geq 0, \tag{3.38}$$

2.

$$\sigma^*_0 = \sigma_0, \tag{3.39}$$

$$\sigma^*_1 = \sigma_1, \tag{3.40}$$

and

3.

$$minimize \sum_{\ell=2}^{L}[\sigma^*_\ell - \sigma_\ell]^2, \tag{3.41}$$

where, σ_ℓ^* is the ℓ^{th} modified cross section moment. The first constraint is the ultimate goal of the moment modification, that is the required positivity of the scattering operator which represents a system of $N \times N$ constraints where N is the quadrature order. The second constraint is the preservation of the momentum transfer via the preservation of the first two cross section moments. This supplies two additional constraints. The third constraint preserves the remaining moments in a least squares fashion. This constraint minimizes the deviation of the modified moments from the original moments over the full range of the expansion. The moment modification problem, then, is to solve the minimization in the third constraint subject to the $N^2 + 2$ conditions proposed by the first two constraints.

The solution of this problem requires use of an optimization computer code tailored to solve exactly such a problem. Lawson and Hanson have done extensive work in the area of linear optimization with constraints, and we have capitalized on their work in solving this problem[20]. Given the M and D operator matrices described previously and the cross section moments, the intended scheme is to generate a new set of moments, subject to the prescribed constraints, using one of Lawson and Hanson's techniques.

Hanson and Haskell have written an appropriate program called WNNLS[21]. It solves two simultaneous sets of linear equations: one set which is exactly satisfied and constrained to positive solutions and another set which is approximately satisfied in a least squares sense. This particular problem requires the definition of the scattering array elements given by equation 3.37 be exactly satisfied and that the elements be positive. Equation 3.37 can be written

$$\sum_{\ell=0}^{L} M_{i\ell} D_{\ell j} \sigma_\ell^* - S_{ij} = 0. \tag{3.42}$$

This satisfies the first constraint of the moment modification. The preservation of the

zeroeth and first cross section moments as exactly satisfied constraints can be written

$$\sigma_0^* - \sigma_0 = 0 \tag{3.43}$$

and

$$\sigma_1^* - \sigma_1 = 0. \tag{3.44}$$

This completes the first set of equations mentioned above. Preserving the remaining moments in a least squares fashion as described by equation 3.41 comprises the second set of equations mentined above and is formulated as

$$\sigma_\ell^* - \sigma_\ell = 0. \tag{3.45}$$

Setting up the constraints in this way fits the equation format required by WNNLS.

Chapter 4

Construction of the scattering operator

4.1 Extraction of low order scattering

A forward peaked cross section can be broken into two parts labelled the smooth cross section and the forward peaked cross section which are defined over the regions of wide angle scatter and small angle scatter, respectively. Such a cross section could be written as

$$\sigma(\mu_o) = \sigma^{smooth}(\mu_o)[\mathcal{U}(\mu_o + 1) - \mathcal{U}(\mu_o - \mu_b)] + \sigma^{F-P}(\mu_o)[\mathcal{U}(\mu_o - \mu_b) - \mathcal{U}(\mu_o - 1)] \quad (4.1)$$

where μ_b is the point where the cross section is broken and $\mathcal{U}$ is the unit step function defined as

$$\begin{aligned} \mathcal{U}(x) &= 0 \qquad , x < 0 \\ &= 1 \qquad , x \geq 0. \end{aligned} \quad (4.2)$$

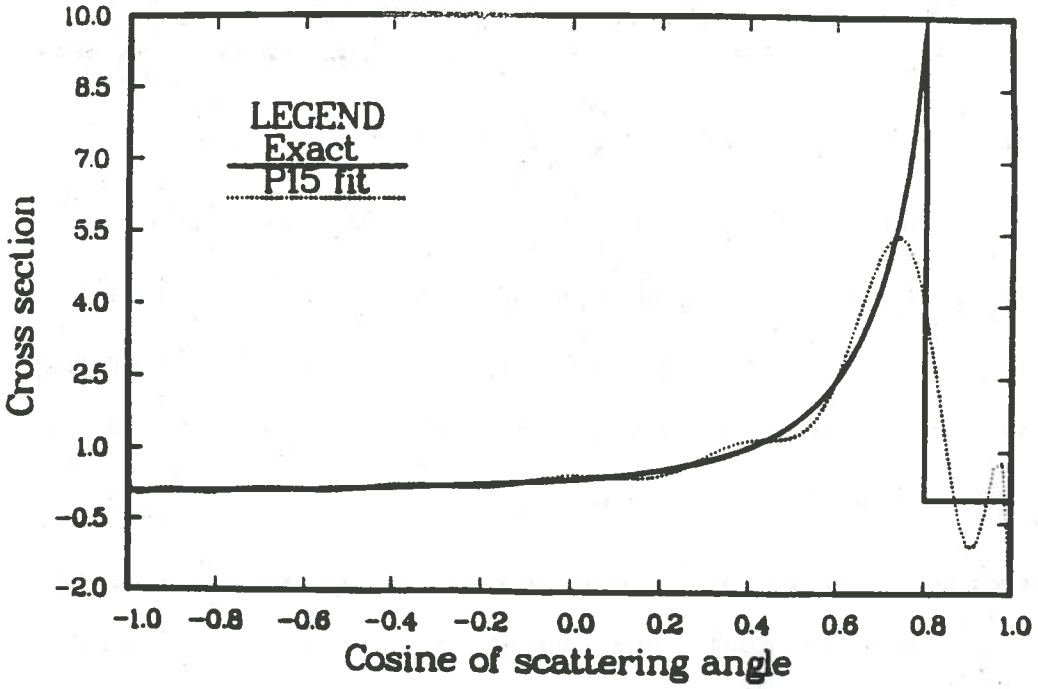

Figure 4.1: Legendre fit of a truncated cross section

The smooth cross section can be expanded in Legendre polynomials of low order, unlike the forward peaked cross section . To expand the smooth cross section in Legendre polynomials , the moments could be calculated in the usual manner:

$$\begin{aligned} \sigma_\ell &= \int_{-1}^{+1} \sigma(\mu_o) P_\ell(\mu_o) d\mu_o \\ &= \int_{-1}^{+1} \sigma^{smooth}(\mu_o)[U(\mu_o + 1) - U(\mu_o - \mu_b)] P_\ell(\mu_o) d\mu_o \quad . \end{aligned} \tag{4.3}$$

This is equivalent to fitting a cross section similar to the one depicted in Figure 4.1 . Attempting to fit the discontinuity at μ_b will degrade the fit over the regions where the quality of fit is important. This is the same problem that is encountered when the smooth and forward peaked regions of the cross section are to be fit simultaneously.

Alternatively, fitting the cross section over the partial range from -1 to μ_b by integrating

over only the partial range:

$$\sigma(\mu_o) = \sum_{\ell=0}^{L} \frac{2\ell+1}{2}\sigma_\ell P_\ell(\mu_o) \quad , \tag{4.4}$$

$$\int_{-1}^{\mu_b} \sigma(\mu_o)P_j(\mu_o)d\mu_o = \sum_{\ell=0}^{L} \frac{2\ell+1}{2}\sigma_\ell \int_{-1}^{\mu_b} P_j(\mu_o)P_\ell(\mu_o)d\mu_o \quad , \tag{4.5}$$

defeats the orthogonality property of the Legendre polynomials since the integral on the right hand side of equation 4.5 does not reduce to $\frac{2}{2\ell+1}\delta_{\ell j}$ as when the integral is performed over the full range. This results in a system of simultaneous equations which can be written

$$\underline{\underline{A}}\,\underline{\sigma} = \underline{B} \quad . \tag{4.6}$$

$\underline{\underline{A}}$ is the matrix operator whose elements are the partial range integrals of the products of Legendre polynomials. $\underline{B}$ is the "source" vector defined as the partial range integrals of the cross section and the Legendre polynomials (the left hand side of equation 4.5). The solution vector, $\underline{\sigma}$, is the desired set of Legendre moments. The drawback to this method lies in the fact that $\underline{\underline{A}}$ approaches singularity as μ_b decreases. When the integral is performed over the full range, $\underline{\underline{A}}$ becomes the identity matrix with a condition number of 1.0 and no inversion of $\underline{\underline{A}}$ is necessary[22]. As the upper limit of the integral is reduced, the condition number increases rapidly to 10^4 for $\mu_b = 0.9$ and 10^7 for $\mu_b = 0.8$. The inversion of $\underline{\underline{A}}$ necessary in solving the matrix equation would entail incurring a loss of four digits of accuracy in the first case and seven digits in the second. This is an unacceptable loss of accuracy, particularly in single precision (8-digit) operations.

A variation on the second method which is still based on a partial range fit would be to transform the Legendre polynomials from the space defined over $(-1,+1)$ to $(-1,\mu_b)$, which effectively defines a set of polynomials orthogonal over $(-1,\mu_b)$. The transformation is performed by evaluating the linear relationship of the two spaces:

$$\mu' = [\frac{\mu_b - 1}{2}] + [\frac{\mu_b + 1}{2}]\mu \quad , \tag{4.7}$$

and substituting it into the Legendre polynomials to define the new orthogonal set, $P'_\ell(\mu')$:

$$P'_\ell(\mu') = P_\ell\{[\frac{\mu_b - 1}{2}] + [\frac{\mu_b + 1}{2}]\mu\} \quad . \tag{4.8}$$

The definition of the moments in the transformed basis would be

$$\sigma'_\ell = \int_{-1}^{+1} \sigma(\mu'(\mu)) P'_\ell(\mu) d\mu \quad . \tag{4.9}$$

The moments are orthogonal on $(-1, \mu_b)$. The discrete ordinates expansion is defined over $(-1, +1)$, so the moments must be transformed back to this space. This can be done by calculating a matrix of projection operators, $\underline{\underline{P}}$, which relates components of σ'_ℓ to σ_ℓ. The projection operators would be

$$P_{\ell j} = \int_{-1}^{+1} P'_\ell(\mu) P_j(\mu) d\mu \quad , \tag{4.10}$$

and the transformation would be

$$\sigma_j = \sum_{\ell=0}^{L} P_{\ell j} \sigma'_\ell \quad . \tag{4.11}$$

The Legendre expansion using these moments would represent the Legendre fit of $\sigma^{smooth}(\mu_o)$ over the range $(-1, \mu_b)$. If the cross section behaves regularly, it should be easy to fit it accurately. Since it is only fit over the partial range, the cross section expansion is not required to behave in a particular way outside the partial range. However, since the smooth region is monotonically increasing, it is not unreasonable to expect the expansion to also be monotonically increasing outside the region of fit similar to the cross section in Figure 4.2 and Figure 4.3. Although, if it is not monotonically increasing, the expansion is still acceptable if it does not oscillate negative.

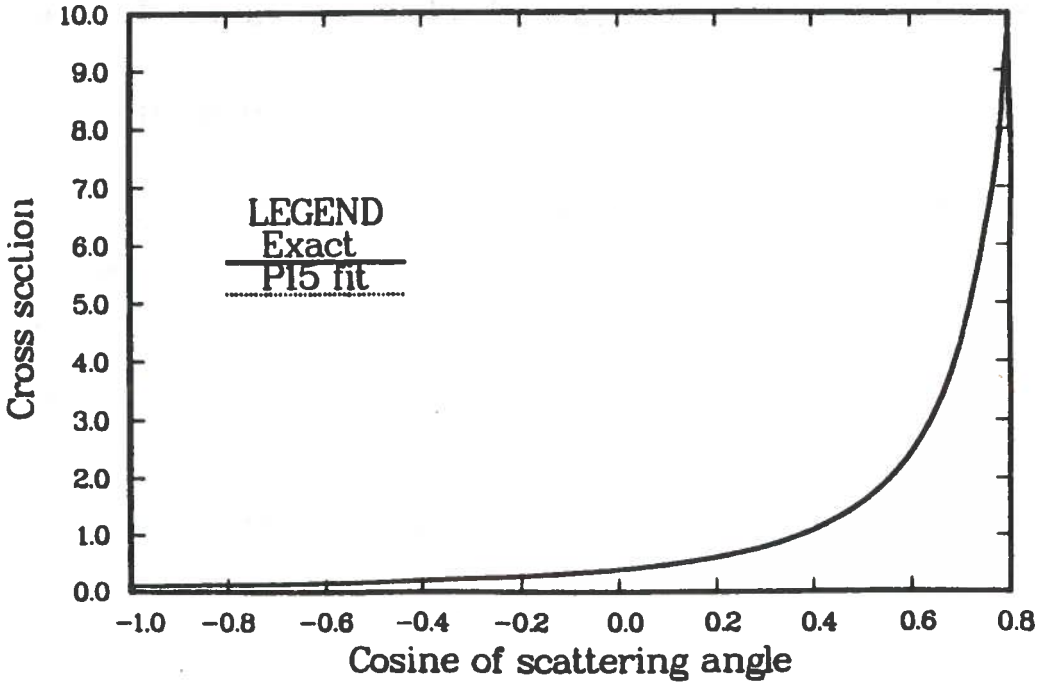

Figure 4.2: Legendre expansion of smooth component in region of fit

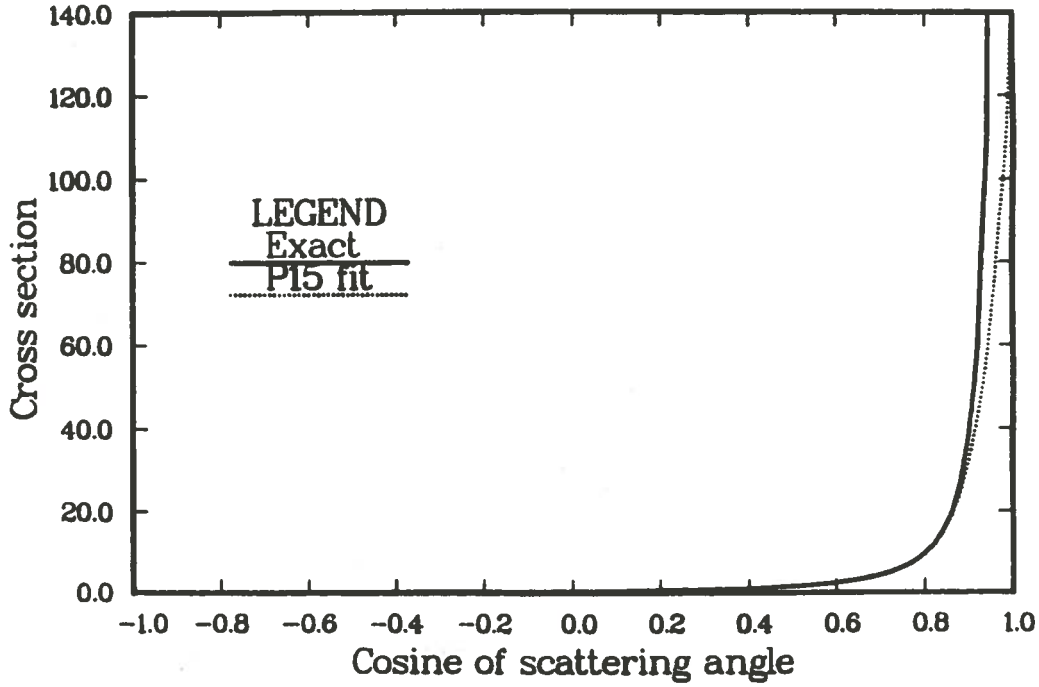

Figure 4.3: Full range Legendre expansion of smooth component

4.2 Evaluation of the forward peaked scattering component

Though the smooth cross section generation technique presented in the preceding section performed the fit over only a partial range, the discrete ordinates scattering operator uses these moments in a full range expansion. The full range behavior of the smooth cross section expansion must be accounted for in calculating the forward peaked cross section moments. Since the momentum transfer is a property of the cross section (see §3.3), it should be preserved in the expansion. If the expansion is written as

$$\sigma(\mu_o) = \sum_{\ell=0}^{L} \frac{2\ell+1}{2} \sigma_\ell P_\ell(\mu_o) \tag{4.12}$$

where

$$\sigma_\ell = \sigma_\ell^{smooth} + \sigma_\ell^{F-P} \quad , \tag{4.13}$$

then

$$\sigma_0 = \sigma_0^{smooth} + \sigma_0^{F-P} \tag{4.14}$$

and

$$\sigma_1 = \sigma_1^{smooth} + \sigma_1^{F-P} \tag{4.15}$$

should be true. The momentum transfer of the cross section is

$$\alpha = \sigma_0 - \sigma_1 \quad , \tag{4.16}$$

which, when the substitution for σ_0 and σ_1 are made, is

$$\alpha = [\sigma_0^{smooth} + \sigma_0^{F-P}] - [\sigma_1^{smooth} + \sigma_1^{F-P}] \quad . \tag{4.17}$$

The terms can be rearranged to give

$$\alpha = [\sigma_0^{smooth} - \sigma_1^{smooth}] + [\sigma_0^{F-P} - \sigma_1^{F-P}] \tag{4.18}$$

$$= \alpha^{smooth} + \alpha^{F-P} \quad . \tag{4.19}$$

Thus, to preserve the momentum transfer of the cross section , the momentum transfer of the forward peaked expansion should be the difference between the exact and smooth expansion momentum transfers.

The forward peaked cross section is represented as the Legendre expansion using the Fokker-Planck equivalent moments. Since the moments are linear in the momentum transfer, they can be calculated by

$$\sigma_\ell(\alpha) = \alpha\sigma_\ell(\alpha = 1) \quad , \tag{4.20}$$

where $\sigma_\ell(\alpha = 1)$ are the values given in Table 1 in the following chapter.

4.3 Composition of full range expansion

The moment representation of the entire cross section is formed by assembling the partial range expansions. If the partial range expansions are

$$\sigma_{smooth}(\mu_o) = \sum_{\ell=0}^{L} \frac{2\ell+1}{2} \sigma_\ell^{smooth} P_\ell(\mu_o) \tag{4.21}$$

and

$$\sigma_{peaked}(\mu_o) = \sum_{\ell=0}^{L} \frac{2\ell+1}{2} \sigma_\ell^{F-P} P_\ell(\mu_o), \tag{4.22}$$

then the full range expansion is

$$\sigma(\mu_o) = \sigma_{smooth}(\mu_o) + \sigma_{peaked}(\mu_o). \tag{4.23}$$

Substituting in the above expansions for the cross sections ,

$$\sigma(\mu_o) = \sum_{\ell=0}^{L} \frac{2\ell+1}{2} \sigma_\ell^{smooth} P_\ell(\mu_o) + \sum_{\ell=0}^{L} \frac{2\ell+1}{2} \sigma_\ell^{F-P} P_\ell(\mu_o), \tag{4.24}$$

the common terms can be brought inside a single summation, giving

$$\sigma(\mu_o) = \sum_{\ell=0}^{L} \frac{2\ell+1}{2}(\sigma_\ell^{smooth} + \sigma_\ell^{F-P})P_\ell(\mu_o). \tag{4.25}$$

Therefore, the ℓ^{th}moment of the full range expansion is the sum of the ℓ^{th}moments of the partial range expansions. This assumes that the relevant regions of each cross section will dominate the other in that region of the expansion. This piecewise generated set of moments is the cross section data supplied to the discrete ordinates computer program.

Chapter 5

Computational results and analysis

This chapter presents two sets of examples as proof of the validity of the modification scheme. First the unmodified and modified Fokker-Planck equivalent moments are presented. Angle-to-angle scattering matrices for two sets of moments of equal order are compared against a finite differences generated scattering matrix. Sample cases using the three matrices show the different results obtained for different dominance ratios. Second, two examples of normally incident electrons on a slab of aluminum are presented. A one MeV incidence case compares results obtained using several variations on the modification technique. A one hundred keV incidence case presents similar results for comparison.

5.1 Comparison of representations of the Fokker-Planck scattering operator

The Fokker-Planck equivalent moments of odd orders are listed in Tables 5.1 and 5.2 for expansion orders three through fifteen. They were generated using equation 3.20 with the momentum transfer normalized to one. Since equation 3.20 was derived by equating the Boltzmann operator and the Fokker-Planck operator, which is only valid for one dimensional slabs or spheres, the moments of order $N-1$ were modified for positivity when used with Gaussian quadratures of order N. Gaussian quadrature sets were chosen since they are the "best" one dimensional integration quadratures. The modified moments are listed with the original moments. Either set can be used by multiplying the moments by the appropriate momentum transfer.

Figure 5.1 shows the cross section expansions using the unmodified and modified P_{15} moments from Table 5.2. Both expansions represent extremely forward peaked scattering probabilities with small wide angle scattering probabilities. Though the scale suppresses it, both expansions oscillate about zero. Upon examining Figure 5.1, one might be led to believe that the original moments would give a positive scattering matrix with an S_{16} Gaussian quadrature since it oscillates less wildly about zero. However, some of the scattering angles lie at points where the expansion oscillates negative. As was required by the least squares modification, none of these scattering angles lie at negative modified expansion points. This can be seen in Figures 5.2 and 5.3 which depict the angle–to–angle scattering matrices using the original and modified moments, respectively. The original discrete scattering operator (Figure 5.2) has negative elements as close as two elements off the diagonal. The flux in this region, even if it is extremely forward peaked, is large and can contribute a large

Table 5.1: Original and modified Fokker-Planck equivalent moments of orders 3 through 11

Moment	Unmodified	Modified	Moment	Unmodified	Modified
P_0	6.0	6.000000000000	P_0	45.0	45.00000000000
P_1	5.0	5.000000000000	P_1	44.0	44.00000000000
P_2	3.0	3.466269038561	P_2	42.0	42.08887236504
P_3	0.0	2.115220398218	P_3	39.0	39.43640494325
P_0	15.0	15.00000000000	P_4	35.0	36.27816672964
P_1	14.0	14.00000000000	P_5	30.0	32.89458669598
P_2	12.0	12.22869048575	P_6	24.0	29.58611341780
P_3	9.0	10.09122757042	P_7	17.0	26.64662271351
P_4	5.0	8.076794615800	P_8	9.0	24.33739270566
P_5	0.0	6.647047639147	P_9	0.0	22.86393289807
P_0	28.0	28.00000000000	P_0	66.0	66.00000000000
P_1	27.0	27.00000000000	P_1	65.0	65.00000000000
P_2	25.0	25.13497797284	P_2	63.0	63.06288071623
P_3	22.0	22.65661842251	P_3	60.0	60.31040270243
P_4	18.0	19.89933392372	P_4	56.0	56.91550239036
P_5	13.0	17.23523099703	P_5	51.0	53.09140484998
P_6	7.0	15.02405724151	P_6	45.0	49.07824755988
P_7	0.0	13.56478190200	P_7	38.0	45.12803882902
			P_8	30.0	41.48888251736
			P_9	21.0	38.38944455697
			P_{10}	11.0	36.02461727527
			P_{11}	0.0	34.54327206652

Table 5.2: Original and modified Fokker-Planck equivalent moments of orders 13 and 15

Moment	Unmodified	Modified	Moment	Unmodified	Modified
P_0	91.0	91.00000000000	P_0	120.0	120.0000000000
P_1	90.0	90.00000000000	P_1	119.0	119.0000000000
P_2	88.0	88.04681279504	P_2	117.0	117.0361955013
P_3	85.0	85.23183677133	P_3	114.0	114.1796399919
P_4	81.0	81.68673624660	P_4	110.0	110.5336401280
P_5	76.0	77.57725779289	P_5	105.0	106.2299951783
P_6	70.0	73.09547872832	P_6	99.0	101.4242242841
P_7	63.0	68.45084431652	P_7	92.0	96.28994971051
P_8	55.0	63.86040646039	P_8	84.0	91.01263719530
P_9	46.0	59.53871227639	P_9	75.0	85.78291506193
P_{10}	36.0	55.68780730776	P_{10}	65.0	80.78970976209
P_{11}	25.0	52.48781376760	P_{11}	54.0	76.21344174388
P_{12}	13.0	50.08851589878	P_{12}	42.0	72.21952335153
P_{13}	0.0	48.60234020080	P_{13}	29.0	68.95239059365
			P_{14}	15.0	66.53027902308
			P_{15}	0.0	65.04093176330

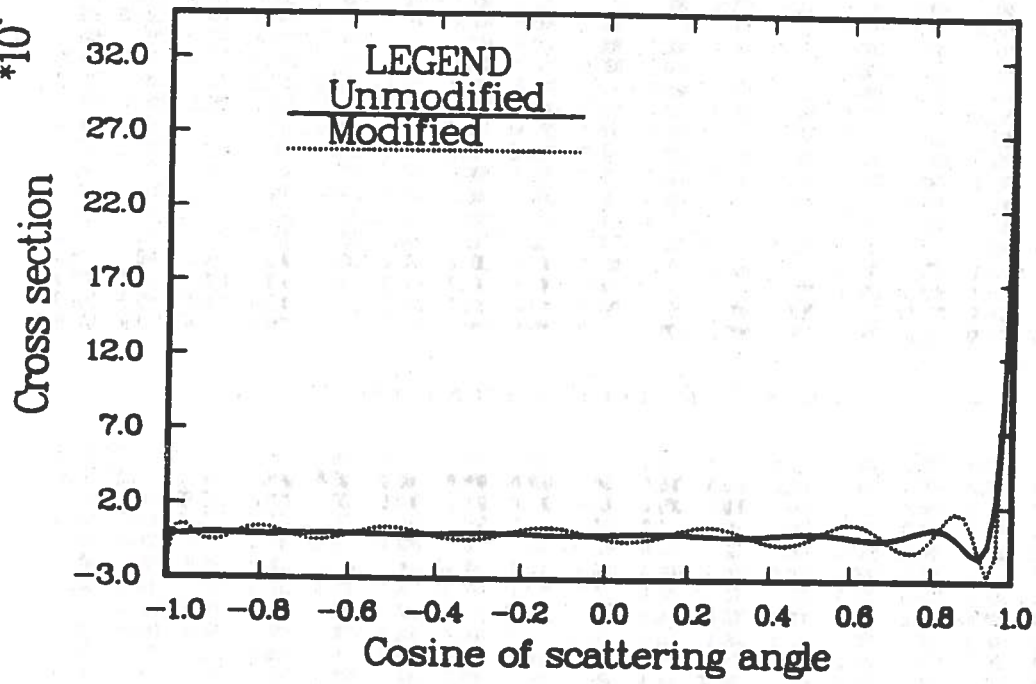

Figure 5.1: P_{15} expansions using Fokker-Planck equivalent moments

90.475	35.924	-8.885	3.723	-1.942	1.141	-0.721	0.477	-0.325	0.224	-0.154	0.104	-0.067	0.040	-0.019	0.005
15.668	77.759	32.609	-8.505	3.749	-2.032	1.227	-0.790	0.528	-0.359	0.245	-0.164	0.105	-0.062	0.030	-0.008
-2.535	21.333	75.996	30.902	-8.041	3.572	-1.951	1.184	-0.762	0.506	-0.338	0.224	-0.143	0.084	-0.041	0.011
0.811	-4.249	23.595	75.443	29.844	-7.573	3.390	-1.844	1.112	-0.708	0.461	-0.299	0.188	-0.109	0.053	-0.015
-0.352	1.560	-5.115	24.863	75.206	29.094	-7.371	3.222	-1.733	1.030	-0.642	0.405	-0.249	0.143	-0.068	0.019
0.183	-0.748	2.009	-5.653	25.721	75.088	28.476	-7.107	3.052	-1.620	0.942	-0.568	0.340	-0.191	0.090	-0.025
-0.107	0.418	-1.017	2.314	-6.039	26.379	75.029	27.946	-6.859	2.903	-1.501	0.844	-0.483	0.264	-0.122	0.033
0.068	-0.260	0.595	-1.213	2.544	-6.346	26.935	75.003	27.444	-6.611	2.734	-1.365	0.732	-0.383	0.173	-0.047
-0.047	0.173	-0.383	0.732	-1.365	2.734	-6.611	27.444	75.003	26.935	-6.346	2.544	-1.213	0.595	-0.260	0.068
0.033	-0.122	0.264	-0.483	0.844	-1.501	2.903	-6.859	27.946	75.029	26.379	-6.039	2.314	-1.017	0.418	-0.107
-0.025	0.090	-0.191	0.340	-0.568	0.942	-1.620	3.052	-7.107	28.476	75.088	25.721	-5.653	2.009	-0.748	0.183
0.019	-0.068	0.143	-0.249	0.405	-0.642	1.030	-1.733	3.222	-7.371	29.094	75.206	24.863	-5.115	1.560	-0.352
-0.015	0.053	-0.109	0.188	-0.299	0.461	-0.708	1.112	-1.844	3.390	-7.573	29.844	75.443	23.595	-4.249	0.811
0.011	-0.041	0.084	-0.143	0.224	-0.338	0.506	-0.762	1.184	-1.951	3.572	-8.041	30.902	75.996	21.333	-2.535
-0.008	0.030	-0.062	0.105	-0.164	0.245	-0.359	0.528	-0.790	1.227	-2.032	3.749	-8.505	32.609	77.759	15.668
0.005	-0.019	0.040	-0.067	0.104	-0.154	0.224	-0.325	0.477	-0.721	1.141	-1.942	3.723	-8.885	35.924	90.475

Figure 5.2: Scattering matrix generated from Morel's unmodified moments

97.944	22.047	0.009	0.000	0.000	0.000	0.000	0.000	0.000	0.000	0.000	0.000	0.000	0.000	0.000	0.000
9.616	92.953	17.418	0.003	0.000	0.000	0.000	0.000	0.000	0.000	0.000	0.000	0.000	0.000	0.000	0.000
0.002	11.395	92.588	16.013	0.001	0.000	0.000	0.000	0.000	0.000	0.000	0.000	0.000	0.000	0.000	0.000
0.000	0.001	12.227	92.480	15.252	0.000	0.000	0.000	0.000	0.000	0.000	0.000	0.000	0.000	0.000	0.000
0.000	0.000	0.001	12.740	92.434	14.825	0.000	0.000	0.000	0.000	0.000	0.000	0.000	0.000	0.000	0.000
0.000	0.000	0.000	0.000	13.111	92.412	14.477	0.000	0.000	0.000	0.000	0.000	0.000	0.000	0.000	0.000
0.000	0.000	0.000	0.000	0.000	13.410	92.401	14.188	0.000	0.000	0.000	0.000	0.000	0.000	0.000	0.000
0.000	0.000	0.000	0.000	0.000	0.000	13.675	92.396	13.929	0.000	0.000	0.000	0.000	0.000	0.000	0.000
0.000	0.000	0.000	0.000	0.000	0.000	0.000	13.929	92.396	13.675	0.000	0.000	0.000	0.000	0.000	0.000
0.000	0.000	0.000	0.000	0.000	0.000	0.000	0.000	14.188	92.401	13.410	0.000	0.000	0.000	0.000	0.000
0.000	0.000	0.000	0.000	0.000	0.000	0.000	0.000	0.000	14.477	92.412	13.111	0.000	0.000	0.000	0.000
0.000	0.000	0.000	0.000	0.000	0.000	0.000	0.000	0.000	0.000	14.825	92.434	12.740	0.001	0.000	0.000
0.000	0.000	0.000	0.000	0.000	0.000	0.000	0.000	0.000	0.000	0.000	15.252	92.480	12.227	0.001	0.000
0.000	0.000	0.000	0.000	0.000	0.000	0.000	0.000	0.000	0.000	0.000	0.001	16.013	92.588	11.395	0.002
0.000	0.000	0.000	0.000	0.000	0.000	0.000	0.000	0.000	0.000	0.000	0.000	0.003	17.418	92.953	9.616
0.000	0.000	0.000	0.000	0.000	0.000	0.000	0.000	0.000	0.000	0.000	0.000	0.000	0.009	22.047	97.944

Figure 5.3: Scattering matrix generated from the modified moments

97.928	22.072	0.000	0.000	0.000	0.000	0.000	0.000	0.000	0.000	0.000	0.000	0.000	0.000	0.000	0.000
9.627	92.942	17.432	0.000	0.000	0.000	0.000	0.000	0.000	0.000	0.000	0.000	0.000	0.000	0.000	0.000
0.000	11.404	92.576	16.021	0.000	0.000	0.000	0.000	0.000	0.000	0.000	0.000	0.000	0.000	0.000	0.000
0.000	0.000	12.232	92.471	15.257	0.000	0.000	0.000	0.000	0.000	0.000	0.000	0.000	0.000	0.000	0.000
0.000	0.000	0.000	12.744	92.428	14.829	0.000	0.000	0.000	0.000	0.000	0.000	0.000	0.000	0.000	0.000
0.000	0.000	0.000	0.000	13.114	92.406	14.480	0.000	0.000	0.000	0.000	0.000	0.000	0.000	0.000	0.000
0.000	0.000	0.000	0.000	0.000	13.413	92.395	14.191	0.000	0.000	0.000	0.000	0.000	0.000	0.000	0.000
0.000	0.000	0.000	0.000	0.000	0.000	13.678	92.391	13.931	0.000	0.000	0.000	0.000	0.000	0.000	0.000
0.000	0.000	0.000	0.000	0.000	0.000	0.000	13.931	92.391	13.678	0.000	0.000	0.000	0.000	0.000	0.000
0.000	0.000	0.000	0.000	0.000	0.000	0.000	0.000	14.191	92.395	13.413	0.000	0.000	0.000	0.000	0.000
0.000	0.000	0.000	0.000	0.000	0.000	0.000	0.000	0.000	14.480	92.406	13.114	0.000	0.000	0.000	0.000
0.000	0.000	0.000	0.000	0.000	0.000	0.000	0.000	0.000	0.000	14.829	92.428	12.744	0.000	0.000	0.000
0.000	0.000	0.000	0.000	0.000	0.000	0.000	0.000	0.000	0.000	0.000	15.257	92.471	12.232	0.000	0.000
0.000	0.000	0.000	0.000	0.000	0.000	0.000	0.000	0.000	0.000	0.000	0.000	16.021	92.576	11.404	0.000
0.000	0.000	0.000	0.000	0.000	0.000	0.000	0.000	0.000	0.000	0.000	0.000	0.000	17.432	92.942	9.627
0.000	0.000	0.000	0.000	0.000	0.000	0.000	0.000	0.000	0.000	0.000	0.000	0.000	0.000	22.072	97.928

Figure 5.4: Scattering matrix generated using a finite difference technique

component to a negative scattering source. The modified scattering operator (Figure 5.3) has no negative elements and is very nearly tridiagonal. The off-diagonal elements are not zero, but of orders varying from 10^{-5} to 10^{-15}, which allows some wide angle scattering. The traditional treatment of the Fokker-Planck operator is a finite difference approximation used to generate the angle–to–angle scattering operator. One of the assumptions in calculating it is that particles can only scatter to the nearest quadrature direction. This causes the finite difference approximation to generate a tridiagonal scattering matrix like the one shown in Figure 5.4 for an S_{16} Gaussian quadrature. Comparison of Figure 5.3 and Figure 5.4 show that the modification caused the discrete scattering operator to approach the finite

Table 5.3: Material properties for three Fokker-Planck scattering problems

Case	α	σ_a
1	0.9	0.1
2	0.1	0.9
3	0.01	0.99

differences representation.

Three normal incidence slab problems were set up to compare the results obtained using the three methods. The medium was a 0.5 centimeter slab with the different properties listed in Table 5.3 for the three different cases. A P_{15} expansion was used with S_{16} Gauss quadrature. A source current of $100\frac{particles}{cm^2-sec}$ was approximated as normally incident by the most forward peaked direction, $\mu = 0.9894$. The reflected angular fluxes for the unmodified, modified, and finite differences scattering matrices are listed in Tables 5.4 through 5.6 for the three cases. Table 5.7 lists the percent reflections.

The first case typifies a highly scattering medium. Sufficient scattering is present to allow significant angular redistribution of the particles. This causes the flux to vary more smoothly in angle, minimizing the importance of the higher order cross section moments. Since the particles scatter more, enough are reflected to prevent a negative reflected angular flux solution (See Table 5.4, column 2). The similarity of the scattering matrices generated with the modified Fokker-Planck equivalent moments and the finite differences approximation causes the flux solutions to be essentially identical. Examination of Table 5.4 shows the differences to be on the order of 0.005 % . This is because the particles scatter frequently enough to overcome the small differences in the wide angle scattering elements.

Table 5.4: Reflected angular fluxes for the first Fokker-Planck scattering problem

Direction Cosine	Unmodified Moments	Modified Moments	Finite Difference
-0.09501	14.429	18.532	18.530
-0.28160	31.855	31.261	31.259
-0.45802	36.902	38.795	38.793
-0.61788	41.416	41.583	41.582
-0.75540	39.401	40.033	40.033
-0.86563	36.282	35.747	35.747
-0.94458	31.215	30.976	30.977
-0.98940	28.304	27.666	27.667

Increasing the amount of absorption causes the different solutions to begin diverging. The results of the second case (Table 5.5) show this. Since the absorption removes a larger number of particles, the wide angle scattering contributes a larger component to the reflected flux. The negative wide angle scattering elements generated with the unmodified moments produced a negative, oscillatory reflected flux solution. The solutions obtained using the modified moments or finite difference scattering matrix are strictly positive and similar, though not as close as for the first case. The nonzero wide angle scattering elements produced by the modified moments are beginning to contribute significantly to the reflected angular flux, causing the solution obtained using this method to be somewhat larger than that of the finite differences technique.

The results of the third case, listed in Table 5.6, show completely divergent sets of results.

Table 5.5: Reflected angular fluxes for the second Fokker-Planck scattering problem

Direction Cosine	Unmodified Moments	Modified Moments	Finite Difference
-0.09501	-2.76250	1.2955E-3†	1.2426E-3
-0.28160	1.32580	2.6187E-3	2.5613E-3
-0.45802	-0.79044	2.7333E-3	2.6923E-3
-0.61788	0.53879	1.4862E-3	1.4686E-3
-0.75540	-0.38398	4.8319E-4	4.7799E-4
-0.86563	0.27983	1.0885E-4	1.0737E-4
-0.94458	-0.20054	2.0539E-5	1.9180E-5
-0.98940	0.12554	4.6186E-6	3.5017E-6

†Read as 1.2955×10^{-3}

Table 5.6: Reflected angular fluxes for the third Fokker-Planck scattering problem

Direction Cosine	Unmodified Moments	Modified Moments	Finite Difference
-0.09501	-1.60910	5.2983E-6	1.2942E-10
-0.28160	0.79383	5.3258E-7	1.8885E-10
-0.45802	-0.49139	2.2953E-7	2.5975E-11
-0.61788	0.32717	1.1130E-8	1.3743E-12
-0.75540	-0.22868	2.1805E-9	4.0908E-14
-0.86563	0.16407	7.9963E-9	8.3631E-16
-0.94458	-0.11633	1.6679E-7	1.3686E-17
-0.98940	0.07239	9.2800E-8	2.2714E-19

Table 5.7: Percent reflections for the three Fokker-Planck scattering problems

Case	Unmodified Moments	Modified Moments	Finite Difference
1	8.9394	9.0343	9.0341
2	-7.2545E-3	2.8145E-4	2.7674E-4
3	-4.4417E-3	7.7367E-8	7.0904E-12

The unmodified moment representation again produced negative results. The modified moment and finite difference techniques have now produced completely different results. Both are positive, but the moment representation produced results several orders of magnitude larger than the finite difference representation. As stated previously, this is due to the wide angle scattering contribution which, in cases of strongly absorbing media, constitutes almost the entire source of reflected particles. When coupled with a smooth scattering cross section expansion, which should dominate the small wide angle scattering elements, these differences between the two positive representations should disappear.

Perhaps the single parameter which best illustrates the differences in all the cases is the reflection, which is listed in Table 5.7 for each case and method. For the first case (highly scattering medium), the three methods produced similar, positive reflections. For the second case (moderately absorbing medium), the unmodified moment representation results in a negative reflection. The modified moment and finite difference representations produce positive reflections which differ by a few percent. For the last case (strongly absorbing medium), the unmodified moment representation again causes a negative reflection. The two positive representations have now diverged, the reflection obtained using the modified moments being larger due to the wide angle scattering.

5.2 Two Rutherford scattering problems

Two similar cases of Rutherford scattering were examined to test the partial range expansion technique coupled with the positive moment representation. The problem was near normally incident ($\mu_1 = 0.98940$) high energy electrons on a slab of aluminum. There were two essential differences in the two cases. The first is the incident energy of the electrons. The incident energy was 1.0 MeV in the first case and 0.1 MeV in the second case. This led

to different scattering and effective absorption parameters. The second difference was the slab thickness. The thickness was 25 mils (0.0635 cm) in the first case and 2.5 mils in the second. The thinner slab allowed some discernable transmission. The scattering model was the Rutherford scattering cross section of the form

$$\sigma_s(\mu_o, E) = \frac{C}{(1 + 2\eta(E) - \mu_o)^2} \quad , \tag{5.1}$$

where C is a material/density factor and η is the so-called "screening factor" due to the orbital electrons in the transport medium. Since there is no absorption in Rutherford scattering, it was mocked up from the removal due to downscatter in energy. The absorption was approximated as

$$\sigma_a = \frac{\beta(E)}{\Delta E} \quad , \tag{5.2}$$

where $\beta(E)$ is the stopping power and ΔE is determined by the energy grid. Using aluminum with parameters:

$$z = 13 \quad ,$$

$$A = 26.9815 \quad ,$$

$$\rho = 2.7 \frac{g}{cc} \quad ,$$

and an energy grid corresponding to fifty groups between 1.0 and 0.1 MeV, the coefficients in Table 5.8 were calculated and used.

The scattering was treated five different ways in both cases. The full range Legendre moments calculated according to equation 2.7 were used to verify a negative flux solution. These moments were modified according the the technique described in section 3.4 and used to determine the solution using modified full range moments. The scattering cross section was fit between -1.0 and 0.8 and these moments were used with three different

Table 5.8: Rutherford cross section parameters

Parameter \ Energy	1.0 MeV	0.1 MeV
C	$0.3902674054 cm^{-1}$	$0.3902674054 cm^{-1}$
η	1.41808402E-5	2.718565583E-4
β	$4.031053963 \frac{MeV}{cm}$	$87.46208032 \frac{MeV}{cm}$
σ_a	$223.9474424 cm^{-1}$	$4859.004462 cm^{-1}$

approximations to the Fokker-Planck differential operator in the remaining three cases. The different approximations were

1. Morel's moments, calculated according to equation 3.20,
2. Morel's moments modified for positivity, and
3. the traditional three point finite difference operator.

The smooth range fits for the two cases are listed in Table 5.9. The different sets of moments for the 1.0 MeV and 0.1 MeV cases are listed in Tables 5.10 and 5.11, respectively. The smooth region moments corresponding to the partial range fit to the cross section are less than 1% of the full range moments or 3% of the piecewise generated moments for the 1.0 MeV cross section and 1.5% and 6%, respectively, for the 0.1 MeV cross section. This shows that the scattering is occurring mainly through angles smaller than 36.87^o, indicating that the scattering is probably forward peaked enough to warrant the Boltzmann-Fokker-Planck treatment. The reflected angular flux solutions, listed in Tables 5.12 and 5.13 and plotted in Figures 5.5 and 5.6, substantiate this claim since the solution obtained with the full range Legendre moments oscillates wildly about zero.

Table 5.9: Smooth region moments of the Rutherford cross section

Moment	1.0 Mev	0.1 MeV
0	10.77560335111	10.68823529807
1	9.3475425386	9.266212240137
2	7.624624279332	7.553407593918
3	5.924741890275	5.865712010444
4	4.406032269297	4.359552453886
5	3.138798128016	3.103983452977
6	2.139361259179	2.114564870424
7	1.391030254064	1.374271639012
8	0.8588198722686	0.848113792851
9	0.5000994544624	0.4936734985579
10	0.2720293838251	0.2684382378124
11	0.1362840991039	0.1344407588309
12	6.1526119624E-2	6.0675442700E-2
13	2.4121883427E-2	2.3781600195E-2
14	7.6365609904E-3	7.5268179769E-3
15	1.6058624069E-3	1.5823787320E-3

Table 5.10: Cross section moments for the 1.0 MeV Rutherford problem

Moment	Legendre	Modified Legendre	Unmodified Fokker-Planck	Modified Fokker-Planck
0	13760.62153659	13760.62153659	315.3931328737	315.3931328737
1	13756.65496695	13756.65496695	311.4265926485	311.4265926485
2	13749.82123209	13748.87377478	304.6267155638	304.7185970988
3	13740.60473474	13737.56446078	295.3113949367	295.7674073578
4	13729.19245164	13723.14903750	283.6387676650	284.9934021435
5	13715.84644502	13706.15320256	269.6791364602	272.8014538978
6	13700.68597485	13687.19595839	253.4488231153	259.6026665521
7	13683.86957645	13666.95797650	234.9311362214	245.8210852427
8	13665.50901853	13646.16365405	214.0910905381	231.8925256867
9	13645.69235018	13625.55428083	190.8860554061	218.2582632992
10	13624.53334647	13605.86499786	165.2731912085	205.3550443715
11	13602.07403769	13587.80309275	137.2141723843	193.6025369356
12	13578.42235004	13572.01963207	106.6776614525	183.3892993411
13	13553.59782372	13559.09323017	73.64002485138	175.0583458605
14	13527.69278088	13549.49752340	38.08482775131	168.8933801809
15	13500.71882667	13543.59363999	1.605862407E-3	165.1066721250

Table 5.11: Cross section moments for the 0.1 MeV Rutherford problem

Moment	Legendre	Modified Legendre	Unmodified Fokker-Planck	Modified Fokker-Planck
0	717.6056358334	717.6056358334	177.7413391577	177.7413391577
1	714.7915066311	714.7915066311	174.9272069009	174.9272069009
2	710.3260824863	710.8431285535	170.4301838570	170.4805719474
3	704.5960075569	704.4834663510	164.5661606770	164.8162391622
4	697.8483668911	697.4645594296	157.4915643252	158.2344496562
5	690.2693802713	689.4103548904	149.2754493301	150.9877369323
6	682.0002186788	681.1504456061	139.9333755546	143.3081604805
7	673.1575288660	672.7403905181	129.4483179314	135.4203963859
8	663.8370332500	664.2261961913	117.7852864946	127.5476432422
9	654.1191277269	655.8118831705	104.9018634109	119.9128586587
10	644.0741099921	647.4081164490	90.75553616176	112.7365363684
11	633.7601758604	639.1437249947	75.30833749565	106.2318740849
12	623.2309422903	631.6533281311	58.52926179356	100.5981382354
13	612.5300884007	624.6524551128	40.39494836627	96.01303882687
14	601.6990048714	619.6903417455	20.88916480043	92.62494024666
15	590.7716560237	615.9246338900	1.582378732E-3	90.54566178682

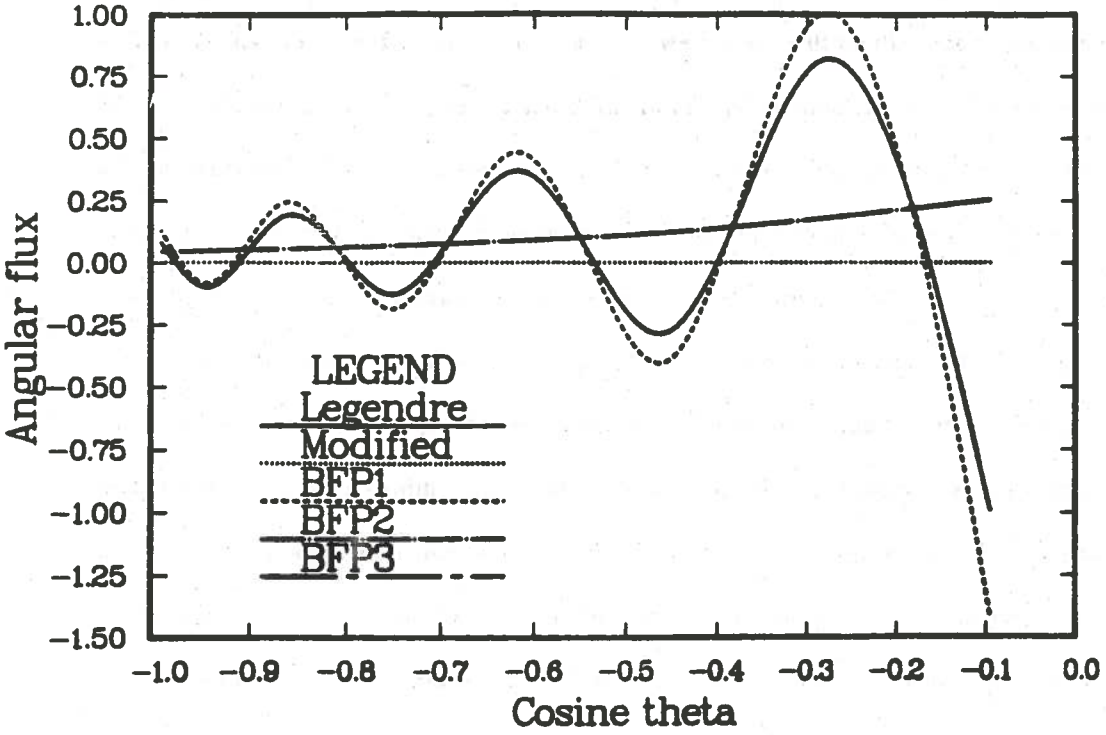

Figure 5.5: Reflected angular fluxes for the 1.0 MeV Rutherford problem

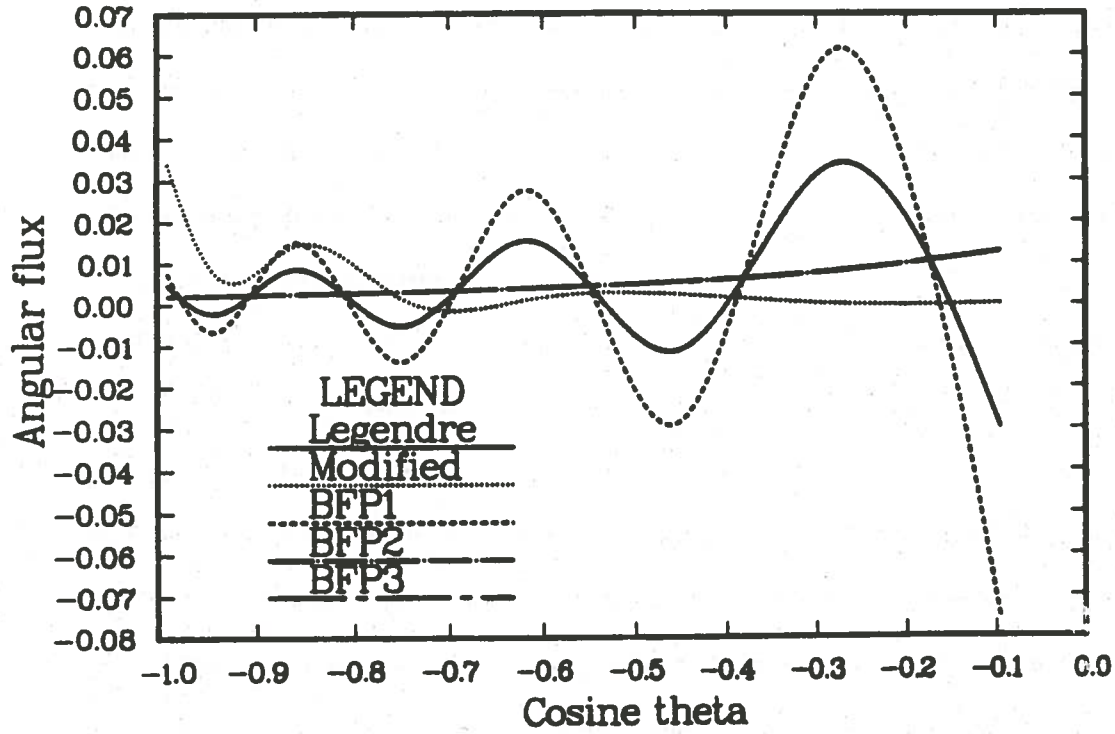

Figure 5.6: Reflected angular fluxes for the 0.1 MeV Rutherford problem

The results obtained for the 1 MeV and 0.1 MeV cases will be discussed together since they are very similar, with the exception of the full range modified moment solutions, which will be explained. As was stated, the solution obtained using the full range Legendre moments oscillates about zero. This proves that the expansion order was too low for the anisotropy of the cross section . Further proof is Figure 1.1 which depicts the exact Rutherford cross section and its full range P_{15} Legendre expansion for the 1 MeV case. The fit is obviously poor for $\mu_o < 0.97$. A first impulse in correcting this might be to simply apply the least squares modification to the full range moments. However, modifying a poor fit for positivity at certain points does not guarrantee a good representation. Depending on the particular features of the poor fit, the expansion may be altered to give almost any result. This is obvious in Figures 5.5 and 5.6. While the plots of the other solutions behave similarly between the two figures, the results using the full range modified moments are markedly different, owing to the different modified scattering matrices. The 1 MeV solution might have been acceptable since it is essentially zero. The 0.1 MeV solution is obviously unrealistic since it oscillates about a solution that is forward peaked in the reverse direction. This reversed peak runs contrary to what is known to be the correct behavior of the solution for the physics of the problem.

The three curves labeled BFP1, BFP2, and BFP3 correspond to partial range moment fits with unmodified Fokker-Planck equivalent moments, modified Fokker-Planck equivalent moments, and the finite differences Fokker-Planck operator, respectively. Comparison of all three curves shows the importance of modifying the Fokker-Planck equivalent moments. The solution obtained using the unmodified moments oscillates more wildly than that of the full range Legendre moments. The off-diagonal scattering elements similar to those in Figure 5.2 (normalized for the appropriate momentum transfer) dominated the elements

of the smooth scattering matrix, causing the solution to oscillate as in the Fokker-Planck scattering problem in the previous section. Modifying the matrix for positivity removes the erratic behavior of the wide angle scattering elements (compare Figure 5.3). Since these elements are small they are dominated by the smooth expansion scattering elements and the Boltzmann-Fokker-Planck operators using the modified moment operator and the finite difference operator become essentially identical, since the majority of the wide angle scattering comes from the smooth cross section expansion. The colinear BFP2 and BFP3 curves in Figures 5.5 and 5.6, being the reflected flux solutions using these two operators, show this. Tables 5.12 and 5.13 show the solutions are identical to five significant digits. A slab geometry Monte Carlo calculation was performed using the 1.0 MeV absorption and scattering cross sections. Due to the extreme forward biasing of the scattering function, one million histories were required to converge the reflected fraction to 2.35E-4 within five percent. This value differs by less than one percent from the one obtained using the modified moments.

5.3 Summary and Conclusions

The full range Legendre fit to a cross section has been shown to be unsatisfactory for extremely anisotropic cross sections and to give inaccurate or nonphysical flux solutions when it is used in transport calculations. Traditional methods of circumventing this problem include expanding the smooth component of the cross section in Legendre polynomials and using a finite difference approximation to the Fokker-Planck continuous slowing down operator to treat the forward peaked scattering. This technique is incompatible with standard discrete ordinates codes which calculate the scattering source based strictly on Legendre expansions. The Boltzmann integral operator using a moment expansion derived by Morel

Table 5.12: Reflected angular fluxes for the 1.0 MeV Rutherford problem

Direction Cosine	Legendre	Modified Legendre	Unmodified Fokker-Planck	Modified Fokker-Planck	Finite Difference
-0.09501	-0.99303	2.67015E-5	-1.4125	0.25445	0.25445
-0.26160	0.81643	6.4241E-6	1.0056	0.17886	0.17886
-0.45802	-0.28352	7.2790E-6	-0.40109	0.12140	0.12140
-0.61788	0.36876	3.2172E-5	0.44386	0.08800	0.08800
-0.75440	-0.12590	1.9234E-4	-0.18530	0.06833	0.06833
-0.86563	0.18778	4.1436E-4	0.24118	0.05658	0.05658
-0.94458	-0.09708	2.3092E-3	-0.08245	0.04977	0.04977
-0.98940	0.083282	1.8452E-3	0.12908	0.04638	0.04638
Reflected Fraction	1.8185E-4	1.2097E-6	1.8637E-4	2.3292E-4	2.3292E-4

Table 5.13: Reflected angular fluxes for the 0.1 MeV Rutherford problem

Direction Cosine	Legendre	Modified Legendre	Unmodified Fokker-Planck	Modified Fokker-Planck	Finite Difference
-0.09501	-0.029904	7.8355E-5	-0.075258	0.012666	0.012666
-0.26160	0.033649	4.1708E-5	0.060909	0.007875	0.007875
-0.45802	-0.011454	0.0024021	-0.029162	0.0053228	0.0053228
-0.61788	0.015398	0.0010589	0.02755	0.003881	0.003881
-0.75440	-0.0051848	0.0019159	-0.013859	0.0030305	0.0030305
-0.86563	0.0084657	0.013791	0.014808	0.0025197	0.0025197
-0.94458	-0.0021748	0.0082238	-0.0065693	0.0022224	0.0022224
-0.98940	0.0046913	0.034103	0.0075713	0.0020742	0.0020742
Reflected Fraction	9.6761E-6	1.5018E-5	8.9835E-6	1.0417E-5	1.0417E-5

has been shown to give equivalent solutions to the Fokker-Planck operator. Since the moment expansion is not everywhere positive, it can lead to negative flux solutions of certain transport problems.

The moments may be modified for an arbitrary quadrature to guarantee a positive flux solution to the transport equation using the modified moments with that quadrature. Sample modifications using Gauss quadratures and Morel's Fokker-Planck equivalent moments have shown that the modification causes the moment generated discrete scattering matrix to approach the finite difference approximation to the Fokker-Planck operator. Sample calculations using the full range Legendre moments, least squares modified Legendre moments, and partial range Legendre moments with Morel's Fokker-Planck equivalent moments, modified sets of Morel's moments, and the finite difference operator have shown that the best results are obtained with the latter two methods and that they are essentially identical.

The smooth region moment expansion coupled with the modified Fokker-Planck equivalent moment expansion is obviously the preferred representation for strongly anisotropic cross sections for use in standard discrete ordinates codes because it is acceptable as input and it guarantees a positive flux solution. However, there are drawbacks associated with both components of the cross section representation. The smooth region expansion requires a partial range fit, which is not always available or easily determined. Extremely complex functions or nonanalytic expressions for the cross section may make a partial range fit difficult. The modification of the moment representation of the Fokker-Planck component of the cross section is quadrature dependent. Moments modified with one quadrature set are only guaranteed to give positive results with that quadrature. They may or may not give positive results with another quadrature and the approximation to the finite difference scattering operator could degenerate. Furthermore, the least squares modification technique

is not guaranteed to give a reasonable solution. Quadratures with a number of directions much larger than the number of moments to be modified (i.e. cylindrical or two dimensional quadratures) may overconstrain the modification, generating a set of nonphysical moments (i.e. $\sigma_\ell > \sigma_0$). However, once the moments have been successfully modified for a particular quadrature, they need only be normalized to the appropriate momentum transfer for any subsequent calculations with that quadrature.

REFERENCES

1. J.J. Duderstadt and W.R. Hamilton, Transport Theory , (New York: John Wiley and Sons, 1979).

2. B.G. Carlson, "The Numerical Theory of Neutron Transport," Methods of Computational Physics , 1 (1963), pp. 1 - 63.

3. George Arfken, Mathematical Methods for Physicists , 3rd. ed. , (New York: Academic Press, 1985), pp. 654 - 55.

4. B.S. Tannenbaum, Plasma Physics , (New York: McGraw-Hill, 1967).

5. J.E. Morel, "Fokker-Planck Calculations Using Standard Discrete Ordinates Transport Codes," Nuclear Science and Engineering , 79 (1981), pp. 340 - 56.

6. Arfken, pp. 652 - 53.

7. Arfken, pp. 693 - 94.

8. Arfken, pp. 694 - 95.

9. Arfken, pp. 968 - 72.

10. E.G. Corman et. al. , "Multigroup Diffusion of Energetic Charged Particles," Nuclear Fusion , 15 (1975), pp. 337 - 86.

11. G.C. Pomraning, "Flux-Limited Diffusion and Fokker-Planck Equations," Nuclear Science and Engineering , 85 (1983), pp. 116 - 26.

12. M.J. Antal and C.J. Lee, "Charged Particle Mass and Energy Transport in a Thermonuclear Plasma," Journal of Computational Physics , 20 (1976), pp. 298 - 312.

13. G.A. Moses, "Laser Fusion Hydrodynamics Calculations," Nuclear Science and Engineering , 64 (1977), pp. 49 - 63.

14. P.A. Haldy and J. Ligou, "A Moment Method for Calculating the Transport of Energetic Charged Particles in Hot Plasmas," Nuclear Fusion , 17 (1977), pp. 1225 - 35.

15. T.A. Mehlhorn and J.J. Duderstadt, "A Discrete Ordinates Solution of the Fokker-Planck Equation Characterizing Charged Particle Transport," Nuclear Science and Engineering , 38 (1980), pp. 86 - 106.

16. M. Caro and J. Ligou, "Treatment of Scattering Anisotropy of Neutrons Through the Boltzmann-Fokker-Planck Equation," Nuclear Science and Engineering , 83 (1983), pp. 242 - 52.

17. Morel, "Fokker-Planck Calculations," pp. 340 - 56.

18. J.E. Morel, "Multigroup Legendre Coefficients for the Diamond Difference Continuous Slowing Down Operator," Nuclear Science and Engineering , 91 (1985), pp. 324 - 31.

19. Arfken, pg. 648.

20. C.L. Lawson and R.J. Hanson, Solving Least Squares Problems , (New York: Prentice-Hall, 1974).

21. R.J. Hanson and K.H. Haskell, "An Algorithm for Linear Least Squares Problems with Equality and Nonnegativity Constraints," Selected Algorithms for the Linear Constrained Least Squares Problem – A Users' Guide , SAND77-0552 (June 1978).

22. Richard L. Burden et. al. , Numerical Analysis , 2nd. ed. , (Boston: Prindle, Weber, and Schmidt, 1981), pp. 396 - 98.

Appendix A

The Boltzmann transport equation

The general Boltzmann transport equation describes a differential balance of particles in phase space(shown in Figure A.1) described by the position vector, $\vec{r}$, the particle energy, E, the direction vector, $\vec{\Omega}$, and the time, t. A simplified version of it describing one group, time independent, one dimensional slab or spherical geometry transport in a nonmultiplying medium is

$$\mu \frac{\partial \psi(x,\mu)}{\partial x} + \sigma_t(x)\psi(x,\mu) = \frac{1}{2\pi}\int_0^{2\pi}\int_{-1}^{+1} \sigma_s(x,\mu_o)\psi(x,\mu')d\mu' d\phi' + Q(x,\mu) \quad , \quad \text{(A.1)}$$

where μ is the cosine of the angle of travel with respect to the x-axis, μ_o is the cosine of the angle of scatter from $\vec{\Omega}'(\phi',\mu')$ to $\vec{\Omega}(\phi,\mu)$, given by

$$\mu_o = \mu\mu' + \sqrt{(1-\mu^2)(1-\mu'^2)}\cos(\phi'-\phi) \quad , \quad \text{(A.2)}$$

and ψ(x,μ) is the particle angular flux density in units of $\frac{particles}{cm^2-sec-steradian}$ at position x, traveling along direction cosine μ.

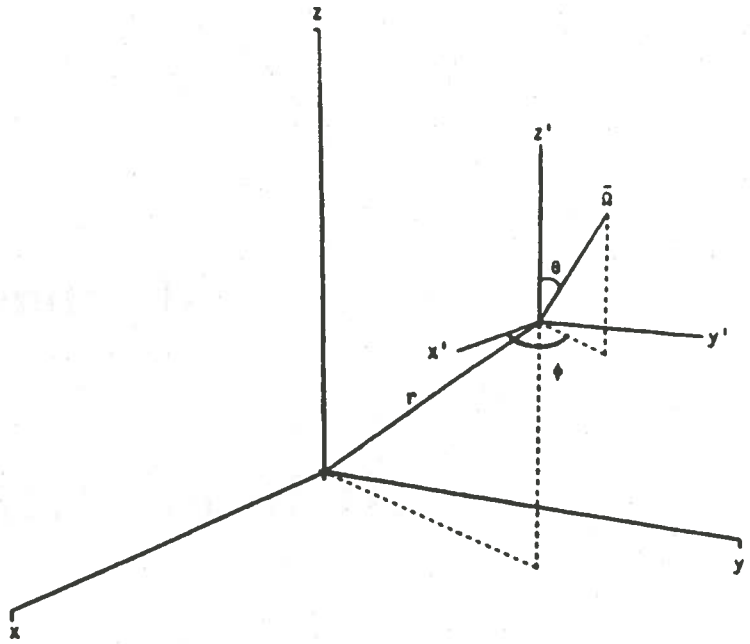

Figure A.1: Standard phase-space coordinate system

The left hand side of equation A.1 represents the loss mechanisms and the right hand side represents the source mechanisms. The first term on the left is the leakage loss per unit volume per second per direction interval. In the next term, σ_t is the macroscopic differential total cross section at position x in units of inverse centimeters. The total loss via collisions with the medium in the angular interval $d\mu$ is $\sigma_t(x)\psi(x,\mu)d\mu$. The coefficient, $\sigma_s(x,\mu_o)$, in the integrand is the macroscopic scattering cross section differential in the initial and final direction cosines, μ' and μ. The integral represents the total number of particles scattering to μ from all directions. The final term represents the fixed source of particles at x about μ.

Appendix B

Derivation of the

Fokker-Planck equation

Figure B.1 shows the direction-space coordinate system. If θ_o is the angle between the initial and final directions, $\vec{\Omega}$ and $\vec{\Omega}'$, then the cosine of the scattering angle, μ_o, is

$$\mu_o = \mu\mu' + \sqrt{(1-\mu^2)(1-\mu'^2)}\cos(\phi'-\phi) \quad . \tag{B.1}$$

If the coordinate system were rotated to align the z-axis and the final direction, $\vec{\Omega}$, as in Figure B.2, the initial direction cosine can be shown to be

$$\mu' = \mu\mu_o + \sqrt{(1-\mu^2)(1-\mu_o^2)}\cos(\phi'-\phi) \quad . \tag{B.2}$$

These important relationships having been established, the actual derivation follows.

The Boltzmann transport equation restricted to a one dimensional slab or sphere, single energy group, time independent, fixed source problem is

$$\mu\frac{\partial\psi}{\partial x} + \sigma_t\psi = \frac{1}{2\pi}\int_0^{2\pi}\int_{-1}^{+1}\sigma_s(\mu_o)\psi(\mu')d\mu'd\phi' + Q \quad . \tag{B.3}$$

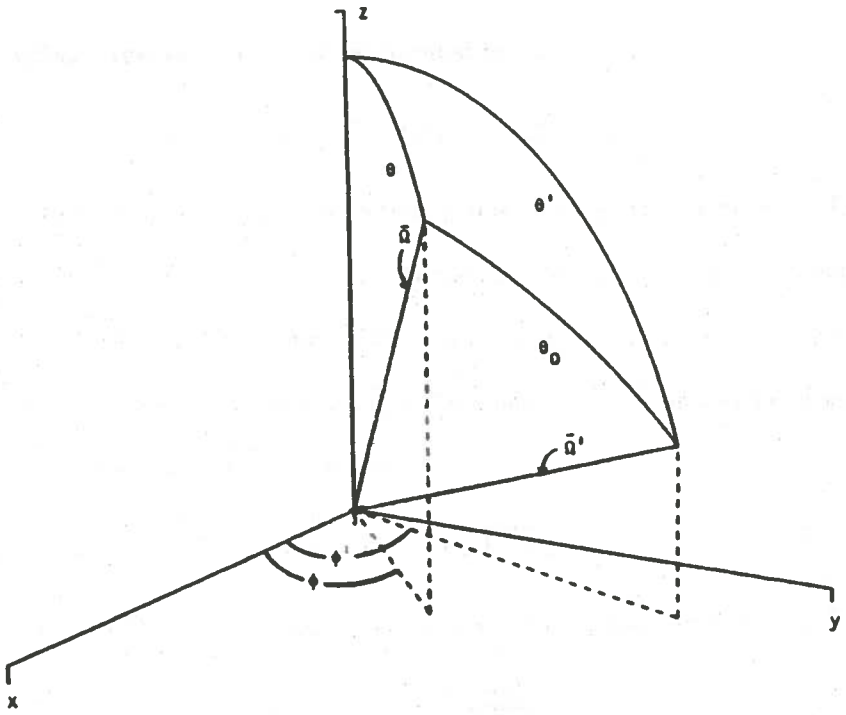

Figure B.1: Direction-space coordinate system

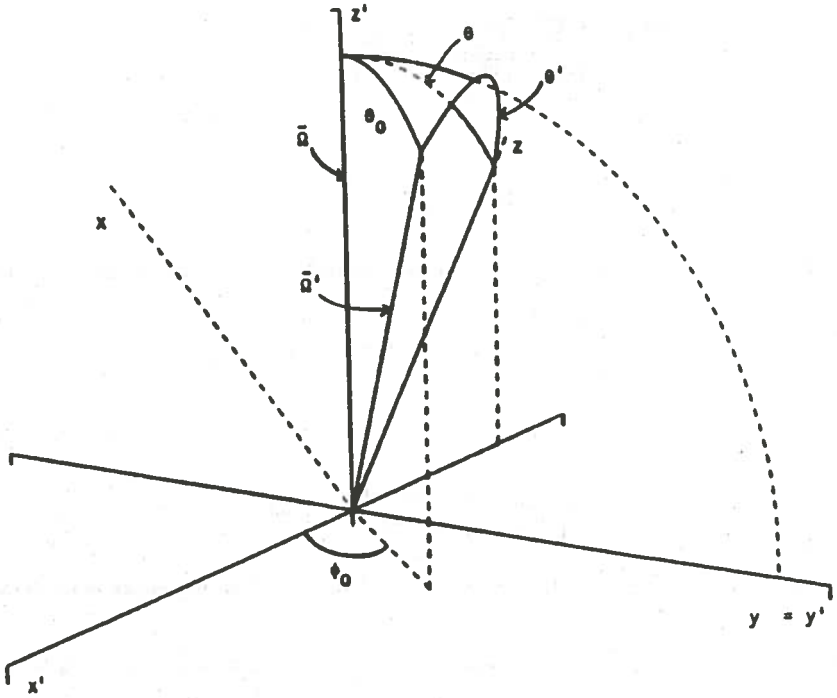

Figure B.2: Rotated direction-space coordinate system

The scattering cross section can be represented by

$$\sigma_s(\mu_o) = \sigma_s \delta(\mu_o - \mu_s) \quad . \tag{B.4}$$

The associated total scattering cross section, cosine of the scattering angle, and momentum transfer are σ_s, μ_s, and $\alpha = \sigma_s(1-\mu_s)$. In the limit as σ_s goes to infinity and μ_s goes to one, α is required to be a constant. This is achieved by defining a new σ_s and μ_s using a dimensionless parameter, ϵ. Since μ_s approaches one, $\sqrt{1-\mu_s^2}$ approaches zero and a new μ_s consistant with this behavior is defined as

$$\sqrt{1-\mu_s^2} \longrightarrow \epsilon\sqrt{1-\mu_s^2} \quad . \tag{B.5}$$

Since α is required to be constant, the scattering cross section is redefined as

$$\sigma_s \longrightarrow \frac{\sigma_s(1-\mu_s)}{1-\sqrt{1-\epsilon^2(1-\mu_o^2)}} \quad . \tag{B.6}$$

Using these definitions, the assumed form of the cross section becomes

$$\sigma_s(\mu_o) = \frac{\sigma_s(1-\mu_s)\delta(\mu_o - \sqrt{1-\epsilon^2(1-\mu_o^2)})}{(1-\sqrt{1-\epsilon^2(1-\mu_o^2)})} \quad . \tag{B.7}$$

Defining

$$\xi = \sqrt{1-\mu_s^2} \tag{B.8}$$

for simplicity and recalling the definition of α,

$$\alpha = \sigma_s(1-\mu_s) \quad , \tag{B.9}$$

then equation B.7 becomes

$$\sigma_s(\mu_o) = \frac{\alpha\delta(\mu_o - \sqrt{1-\epsilon^2\xi^2})}{(1-\sqrt{1-\epsilon^2\xi^2})} \quad . \tag{B.10}$$

Using these new expressions for σ_s and $\sigma_s(\mu_o)$, the Boltzmann transport equation becomes

$$\mu\frac{\partial\psi}{\partial x} + \sigma_a\psi + \frac{\alpha\psi}{1-\sqrt{1-\epsilon^2\xi^2}} = \frac{\alpha}{2\pi(1-\sqrt{1-\epsilon^2\xi^2})} \times \int_0^{2\pi}\int_{-1}^{+1} \delta(\mu_o - \sqrt{1-\epsilon^2\xi^2})\psi(\mu')d\mu' d\phi' + Q \quad . \tag{B.11}$$

Since the δ-function is in terms of μ_o, the variables of integration must be changed from (μ', ϕ') to (μ_o, ϕ_o). This is done by transforming from the laboratory system to the scattering system(shown in Figure A.3). This corresponds to the coordinate rotation described earlier. Making this substitution and integrating over μ_o, the form of the transport equation becomes

$$\mu\frac{\partial\psi}{\partial x} + \sigma_a\psi + \frac{\alpha\psi}{1-\sqrt{1-\epsilon^2\xi^2}} = \frac{\alpha}{2\pi(1-\sqrt{1-\epsilon^2\xi^2})}\int_0^{2\pi}\psi(\mu')d\phi_o + Q \quad , \tag{B.12}$$

where the previous definition of μ',

$$\mu' = \mu\mu_o + \sqrt{(1-\mu^2)(1-\mu_o^2)}\cos(\phi'-\phi) \quad , \tag{B.13}$$

becomes

$$\mu' = \mu\sqrt{1-\epsilon^2\xi^2} + \xi\epsilon\sqrt{1-\mu^2}\cos(\phi'-\phi) \tag{B.14}$$

using the new, asymptotic definition of μ_o.

To perform the integration over ϕ_o, the flux, $\psi(\mu')$, is expanded in a Maclaurin series in ϵ,

$$\psi(\mu') = \psi(\mu) + \frac{\partial\psi}{\partial\epsilon}_{\epsilon=0}\epsilon + \frac{\partial^2\psi}{\partial\epsilon^2}_{\epsilon=0}\frac{\epsilon^2}{2} + O(\epsilon^3) \quad , \tag{B.15}$$

where the derivatives can be evaluated using the chain rule:

$$\frac{\partial\psi}{\partial\epsilon} = \frac{\partial\psi}{\partial\mu}\frac{\partial\mu}{\partial\mu'}\frac{\partial\mu'}{\partial\epsilon} \quad . \tag{B.16}$$

Evaluating the derivatives and substituting them into equation B.15 , the flux expansion becomes

$$\begin{aligned}\psi(\mu') = \quad & \psi(\mu) + \tfrac{\partial\psi}{\partial\mu}\xi\epsilon\sqrt{1-\mu^2}\cos\phi_o + \\ & \tfrac{1}{2}[\tfrac{\partial^2\psi}{\partial\mu^2}\xi^2(1-\mu^2)\cos^2\phi_o - \tfrac{\partial\psi}{\partial\mu}\mu\xi^2]\epsilon^2 + O(\epsilon^3) \quad .\end{aligned} \tag{B.17}$$

Substituting this expression into equation B.12 and integrating over ϕ_o, the following equation results:

$$\mu\frac{\partial\psi}{\partial x}+\sigma_a\psi+\frac{\alpha\psi}{1-\sqrt{1-\epsilon^2\xi^2}}= \frac{\alpha}{2\pi(1-\sqrt{1-\epsilon^2\xi^2})}\times \{2\pi\psi+\frac{\epsilon^2}{2}[\frac{\partial^2\psi}{\partial\mu^2}\xi^2(1-\mu^2)\pi-\frac{\partial\psi}{\partial\mu}\mu\xi^2 2\pi]+O(\epsilon^3)\}+Q \tag{B.18}$$

Subtracting $\frac{\alpha\psi}{1-\sqrt{1-\xi^2\epsilon^2}}$ from both sides, cancelling common factors of π, and noting that

$$\frac{\partial}{\partial\mu}(1-\mu^2)=-2\mu \quad , \tag{B.19}$$

the expression in curly braces can be rewritten, giving

$$\mu\frac{\partial\psi}{\partial x}+\sigma_a\psi=\frac{\alpha}{4(1-\sqrt{1-\epsilon^2\xi^2})}[\frac{\partial}{\partial\mu}(1-\mu^2)\frac{\partial\psi}{\partial\mu}\xi^2\epsilon^2+O(\epsilon^3)]+Q \quad . \tag{B.20}$$

In the required limit ($\epsilon=0$), the following holds true:

$$\frac{lim}{\epsilon\to 0}\frac{1}{1-\sqrt{1-\xi^2\epsilon^2}}=\frac{2}{\xi^2\epsilon^2} \quad . \tag{B.21}$$

Then in the Fokker-Planck limit, equation B.20 becomes

$$\mu\frac{\partial\psi}{\partial x}+\sigma_a\psi=\frac{2\alpha}{4\xi^2\epsilon^2}[\frac{\partial}{\partial\mu}(1-\mu^2)\frac{\partial\psi}{\partial\mu}\xi^2\epsilon^2+O(\epsilon^3)]+Q \quad . \tag{B.22}$$

Cancelling $\xi^2\epsilon^2$ in the numerator and denominator reduces the order of error from third to first, resulting in the final form of the Fokker-Planck approximation to equation B.3 :

$$\mu\frac{\partial\psi}{\partial x}+\sigma_a\psi=\frac{\alpha}{2}\frac{\partial}{\partial\mu}(1-\mu^2)\frac{\partial\psi}{\partial\mu}+Q+O(\epsilon) \quad . \tag{B.23}$$

Vita

Mark Landesman was born in Wichita, Kansas, on December 5, 1960 to Robert and Margaret Landesman. He attended high school at Salmen in Slidell, Louisiana, and was graduated in 1979.

He entered Louisiana State University in 1979 and began studying mechanical engineering. He received his B.S. in 1984 and entered Graduate School there in the Department of Nuclear Engineering.